# CURRENT OSCILLATIONS IN SEMI-INSULATING Cr-DOPED GALLIUM ARSENIDE

by

P. W. F. LENCZEWSKI

Dissertation submitted to the Faculty of Graduate Studies
of the University of Ottawa in partial fulfillment
of the requirements for the degree
Master of Science

1973

© P.W.F. Lenczewski, Ottawa, 1973.

ABSTRACT

Low frequency ($10^{-1}$ - $10^{2}$ Hz) current oscillations due to field dependent trapping were studied in Cr-doped high resistivity GaAs. Electrical conductivity in the dark as a function of temperature and photoconductivity around 90°K and 300°K were studied under both low and high field conditions.

The energies of some dominant impurity levels were determined. Particular importance was attached to the photoconductivity generated by 0.90μ radiation. Its generation was explained in terms of a model based on double excitation and an energy level diagram containing four impurity levels, one of which acted as a sensitizing centre

The dependence of the current oscillations on a number of controlling parameters was studied in the temperature range 90°K to 300°K. The threshold field, intensity of 0.90μ radiation, and threshold temperature were three of these parameters, and they yielded a value of minimum $n\ell$ product needed for the generation of oscillations that indicated the mechanism responsible was field dependent trapping.

Optical and temperature quenching of the oscillations was used to identify one particular impurity level as being responsible for the oscillatory behaviour of the material. This level was found to be 0.45 eV above the valence band, and also acted as both the compensating level and the sensitizing centre in the material.

An original two source experiment was performed to confirm that the 0.45 eV level was responsible for the field dependent trapping mechanism.

UNIVERSITY OF OTTAWA

ACKNOWLEDGEMENTS

The author wishes to thank Dr. E. Fortin for his support, guidance and encouragement during the course of this work. Thanks are also due to Dr. J. Basinski, Mr. R. Glinski and Mr. R. Senechal for helpful suggestions and discussions.

The capable and prompt attention of all the workshop staff is gratefully acknowledged, as well as the able assistance of Mr. R. Hart. Thanks is also due to Miss L. Sawyer for typing this manuscript.

I would like to express my thanks to my wife, Sandra, for her patience during the course of this work.

Finally, financial assistance in the form of an Ontario Government Graduate Fellowship is greatfully acknowledged.

VANIER LIBRARY
UNIVERSITY OF OTTAWA

LIST OF ILLUSTRATIONS

Page

Figure 2-1 Schematic Diagram of Potential Around a Negatively Charged Impurity Centre 12

2-2 Current-density (J) vs. Electric Field (E) Characteristics for Voltage Controlled N.D.R. 14

2-3 Formation of High-Field Domain in a Voltage Controlled N.D.R.. 14

2-4 Formation of a Domain in a Perturbed Medium of Negative Resistivity 17

2-5 Excitation and Recombination Processes in a Photoconductor with Fast and Slow Recombination Centres. 20

3-1 GaAs Sample with Indium Contacts 25

3-2 Cross-section of Optical Cryostat 26

3-3 Schematic Block Diagram of Apparatus 28

3-4 Experimental Arrangement-Single Source 29

3-5 Experimental Arrangement-Double Source 29

3-6 Calibration Curve for Bausch and Lomb Monochromator A 32

3-7 Calibration Curve for Bausch and Lomb Monochromator B 33

3-8 Intensity Calibration 35

UNIVERSITY OF OTTAWA LIBRARY

| | | Page |
|---|---|---|
| 4-1 | I-V Characteristics at $300^{\circ}$K | 40 |
| 4-2 | I-V Characteristics at $90^{\circ}$K | 42 |
| 4-3 | Dark Current as a Function of Temperature Under Low and High Field Conditions | 43 |
| 4-4 | Photocurrent-Electric Field Characteristics at $90^{\circ}$K | 47 |
| 4-5 | Spectral Response at $300^{\circ}$K for High and Low Field Conditions | 50 |
| 4-6 | Spectral Response at $90^{\circ}$K under Low Field Conditions-Scan Up | 53 |
| 4-7 | Spectral Response at $90^{\circ}$K under Low Field Conditions-Scan Down | 54 |
| 4-8 | Photocurrent as a Function of Temperature Under Low Bias Condition for Various Wavelengths | 55 |
| 4-9 | Model for Double Excitation and Sensitizing Mechanism in GaAs. | 57 |
| 4-10 | Energy Distributions for Impurity Levels in Semi-insulating GaAs at $300^{\circ}$K and $90^{\circ}$K. | 62 |
| 4-11 | Photocurrent as a Function of Temperature Under High Field Conditions | 63 |
| 4-12 | Temperature Dependence of the Period of Oscillation | 67 |
| 4-13 | Frequency of Oscillation as a Function of Intensity at $90^{\circ}$K | 76 |

Page

4-14 Maximum Photocurrent as a Function of Intensity at 90°K 71

4-15 Spectral Response at 90°K Under High Field Conditions 73

4-16 Frequency of Oscillation as a Function of Applied Electric Field at 300°K 75

VANIER UNIVERSITY OTTAWA

LIST OF TABLES

Page

Table 4-1 Variation of Minimum $n\ell$ Product with Temperature 65

4-2 Impurity Levels in GaAs as Found in This Work 81

4-3 Characteristics of Three Types of Oscillations in GaAs 82

VANIER LIBRARY UNIVERSITY OF OTTAWA

TABLE OF CONTENTS


| | | | Page |
|---|---|---|---|
| Abstract | | | ii |
| Acknowledgements | | | iii |
| List of Illustrations | | | iv |
| List of Tables | | | vii |
| Chapter I | | INTRODUCTION | 1 |
| | I-1 | Origin of Project | 1 |
| | I-2 | Method of Study | 2 |
| | I-3 | Plan of Thesis | 4 |
| Chapter II | | THEORY | 6 |
| | II-1 | Negative Differential Resistance | 7 |
| | | 1.1 Gunn Effect | 7 |
| | | 1.2 Acoustoelectric Effect | 8 |
| | | 1.3 Field Dependent Trapping | 10 |
| | | 1.4 Other Effects | 13 |
| | II-2 | High Field Domains | 13 |
| | II-3 | Optical Sensitizing Centres | 19 |
| Chapter III | | EXPERIMENTAL MATERIAL, EQUIPMENT AND PROCEDURE | 22 |
| | III-1 | Material and Equipment | 22 |
| | | 1.1 Some Properties of GaAs | 22 |
| | | 1.2 Sample Preparation | 23 |
| | | 1.3 General Apparatus | 24 |

Page

III-2 PROCEDURE 30

2.1 Electrical and Optical Properties 30

2.2 Current Oscillations and Quenching 34

CHAPTER IV RESULTS AND DISCUSSION 38

IV-1 Electrical Properties 38

1.1 I-V at $300^{o}K$ 38

1.2 I-V at $90^{o}K$ 41

1.3 Variation of Dark Current with Temperature 44

IV-2 Optical Properties 46

2.1 $I_p$-V Characteristics 46

2.2 Spectral Response 49

2.3 Variation of Photocurrent with Temperature for Selected Wavelengths 52

2.3.1 0.90μ 56

2.3.2 1.16μ 58

2.3.3 1.30μ 60

2.4 Energy Levels 61

IV-3 Current Oscillations and Quenching 61

3.1 Dependence of the Current Oscillations on

3.1.1 Temperature 61

A - Photocurrent 61

B - Period 66

3.1.2 Intensity of Illumination 69

3.1.3 Wavelength of Illumination 72

3.1.4 Electric Field 74

UNIVERSITY OF OTTAWA

Page

3.2 Quenching 74

3.2.1 Optical Quenching 74

3.2.2 Thermal Quenching 78

3.2.3 Quenching by a Second Source 79

IV-4 Summary of Results 80

CHAPTER V CONCLUSION 83

Appendix 86

List of References 96

VANIER LI
UNIVERSITY

# CHAPTER I INTRODUCTION

## I-1 Origin of Project

Low frequency current oscillations in semi-insulating Cr-doped GaAs were first observed in these laboratories by H. M. Brown and E. Fortin during the study of intrinsic photoconductivity and surface effects of the material (69M1, 69M2). These oscillations ($10^{-1}$ - $10^{2}$ Hz) were found to occur at $90^{\circ}$K for applied fields greater than 750 V/cm and initially only when the sample was illuminated by 0.90μ radiation.

A search of the then current literature indicated that this anomalous behaviour was not unique to the samples being used, but had been reported by other authors, not only for Cr-doped GaAs (69I1, 69V1), but also for high resistivity GaAs doped with copper (61B1), oxygen (63B1, 66K1, 67T1, 68T1, 69V2), and also GaAs compensated by irradiation of fast neutrons (68S1, 69S1). While a theory had been proposed to explain such behaviour in a semiconductor (61R1, 61R2, 61R3, 63R1), the fact that the oscillations in GaAs would occur for different compensating agents, as well as the fact that GaAs contains a large number of impurity levels (an important factor in generating the oscillations), many of them little known, made it difficult to determine the actual mechanism responsible for the oscillations.

With these two facts in mind, it was then decided that a systematic study of the oscillations would be undertaken, with the aim of determining the impurity level or levels in the GaAs that were directly responsible for the oscillations. Also, if the research proved fruitful,

a possible mechanism explaining this particular behaviour of the material would be proposed. It was also felt that such an investigation would contribute to (or at least confirm) the knowledge of the energy values of the impurity levels in the material (experimental results were published at the end of the research period (70L1)).

Finally, it should be mentioned that during the investigation of the current oscillations, a second anomalous effect was encountered in the material, that of photoconduction "memory", and this was subsequently investigated by F. Prat (72P3) and eventually served as the material for his thesis (72P4).

## I-2 Method of Study

The investigation of the current oscillations in the GaAs was divided into two main areas of study.

First, a determination of some of the electrical and optical properties of the material, with particular attention to:

- the I-V characteristics of the sample, both in the dark and under illumination;
- the temperature dependence of the current; and
- the spectral response of the sample in the range of 0.7μ to 1.6μ.

This allowed the determination of some of the impurity levels in the material, as well as furnishing initial data on the oscillations.

Second, a investigation of chosen parameters affecting the creation and quenching of the current oscillations in the GaAs. These

UNIV ... OTTAWA

parameters were:

- temperature of the sample;
- intensity of the incident radiation;
- wavelength of the incident radiation;
- electric field applied to the sample; and
- previous optical history of the sample.

Finally, as a method of substantiating the results obtained by the above procedure, a two source (optical) experiment was performed.

While the results in general confirmed the published information for current oscillations in GaAs (previously mentioned references plus 70T1, 70T2, 71V1, 72B1, 72P2), the following three points were of particular interest:

1) The determination of the 0.45 eV impurity level as the one responsible for the oscillatory mechanism;

2) The importance of the above mentioned level being partly filled with electrons if current oscillations were to be generated; and

3) The determination of an original experiment (two source experiment) to verify which level was responsible for the oscillations.

After the results were organized and studied, two objectives were attained:

1) A simple energy level diagram of the impurity levels in the material was determined; and

2) A mechanism explaining the current oscillations in terms of the above energy level diagram was presented.

## I-3 Plan of Thesis

The first part of this thesis (Chapter II) deals primarily with the theory of current oscillations, with a brief outline of the mechanisms that have been proposed to explain such oscillations. Since Field Dependent Trapping is the mechanism responsible for the oscillations observed in this work, a more extensive presentation of this theory, as originally proposed by Ridley and Watkins (61R1, R2, R3) is given in an Appendix at the end of the thesis. The section on current oscillations ends with a description of travelling high field domains in a material, these being the actual oscillations.

The latter part of the chapter briefly describes the effect that sensitizing centres can have on a photoconductor, in particular on carrier generation, a critical parameter in generating the current oscillations.

The following Chapter (III) describes the experimental material and equipment used in this research, and details the procedures followed.

Chapter IV gives the results of this research and discusses them. It is divided into four main sections:

1) electric properties,
2) optical properties,
3) current oscillations and quenching,
4) summary of results

In each section the results are presented and then discussed. Since in some cases a particular result may apply to more than one section, there occurs the occasional overlap; however, the results have been presented

as systematically as possible.

Finally, the concluding Chapter briefly restates the major accomplishments of this work and proposes a number of practical applications for the effect studied.

## CHAPTER II THEORY

At low temperatures and under high electric fields, high resistivity GaAs, when illuminated with radiation of certain wavelengths in the I.R., becomes unstable and "generates" current oscillations in the circuit. These oscillations are attributed to a mechanism initiated by the appearance of Negative Differential Resistivity (from here on referred to as N.D.R.) in the sample. The first part of this Chapter, then, will describe the most common causes of N.D.R. in a material such as GaAs, including the one actually responsible for the oscillations in this case: Field Dependent Trapping (from here on referred to as F.D.T.).

The second part of this Chapter will describe the effects of having a region of N.D.R. in the sample;the formation and travel of high field domains which traverse the sample from cathode to anode and thus register as current oscillations in the monitoring circuit.

Because the formation of high field domains is partly dependent on the free carrier concentration, and the free carriers in this work were optically generated, the last part of this Chapter will deal with impurity centres (sensitizing centres) that can optically affect such carrier concentrations. Also, these sensitizing centres are of special importance in this work since they were found to be responsible for F.D.T.

## II-1 Negative Differential Resistance (N.D.R.)

### 1.1 - Gunn Effect

While oscillatory current behaviour had been observed in GaAs (and other semiconductors) prior to 1961, it wasn't until Ridley and Watkins (61R1) proposed that N.D.R. could be generated under certain conditions in a material that a more systematic study of this phenomenon was undertaken. The model was based on a material that had a conduction band with two subsidiary sub-bands separated by a certain energy difference (as is the case with GaAs). The N.D.R. arose when, under the influence of a high electric field parallel to a principal axis of the crystal, the charge carriers (electrons) in the conduction band were accelerated, and their effective temperature rose above the lattice temperature. The net effect was an alteration in both the mobility and electron density in the bands. The result was a transfer of electrons from a high mobility, low effective mass centre valley to a low mobility, high effective mass satellite valley. When this occurred, the drift velocity as a function of applied electric field decreased, thus yielding a region in the I-V characteristics of the material where an increase in applied field resulted in a decrease in current, or N.D.R.

The presence of N.D.R. in the material gave rise to the formation of high field domains at one place or nucleation point in the crystal (assuming the crystal was long enough), and the domain would travel across the crystal and produce a current drop while in transit. After the disappearance of the domain at the anode (corresponding to the electrons falling back to the centre valley), a new domain would form

near the cathode. This process, when repeated, manifests itself in current oscillations, and a more detailed description of the domains will be given in a latter part of this Chapter (sec. 2).

Gunn discovered current instabilities in GaAs which he initially could not explain (64G1). Further experiments, however, confirmed that, the theory developed by Ridley and Watkins, and independently by Hilsum (62H2) in 1962, was the correct explanation of the behaviour. The now familiar Gunn oscillations, which are typically in the GHz region for GaAs (due to domain velocities > $10^7$ cm/sec), are obtained for applied fields above about 1.5 kV/cm. These values greatly exceed the values typical of the oscillations in this work. Thus the Gunn effect is not believed responsible for the effect observed in this study. The next mechanism to be discussed, however, yields results closer to those obtained in this research.

## 1.2 - Acoustoelectric Effect

A second mechanism that can induce N.D.R. and thus the formation of travelling high field domains in a material is the acoustoelectric effect (57W1). Under normal conditions, in a semiconductor such as GaAs, a low applied D.C. field will induce a drift velocity to the electrons in the conduction band which will be small in comparison to the wave velocity of the phonons. In this case, the electrons on the one hand and the phonons on the other, can be treated as independent systems, and any coupling between them as a small perturbation.

If, however, the applied field is increased to the point where

the drift velocity exceeds the wave velocity of the phonons ($3.0 \times 10^5$ cm/sec in GaAs), then the two systems are no longer independent.

The net effect can be illustrated by considering the basic mechanism (62S2). When the drift velocity of the electrons exceeds the velocity of sound, acoustic waves in the crystal gain energy from the field and a growing hypersonic wave is generated (amplification). If the amplitude of the sound wave is sufficiently large, the potential difference between crest and trough will exceed kT and substantially all of the free carriers will be bunched in the potential trough (free space charge) and the local deformation potential, or piezoelectric fields, will exceed the applied field. Increasing the electric field under these conditions will push the electrons harder against the walls of their potential troughs and will increase the power going into the sound wave without causing the electrons to drift faster than the sound wave. Thus for sufficiently high applied field, the acoustoelectric current will be sufficiently large to make it comparable in magnitude to the ohmic current. The result will be a partial cancellation of the ohmic current which will show up as a deviation from Ohm's Law in the I-V characteristics of the crystal. The change will be a decrease in the current for increasing field (above the threshold field) yielding a region of N.D.R. In analogy to the "transferred electron theory" of the Gunn oscillations, the acoustoelectric effect describes the net transfer of carrier energy and drift momentum to the acoustic flux, which must culminate in a decrease in the carrier mobility for increasing applied fields.

Current oscillations due to travelling domains formed through

this effect have been observed in a number of materials (62S2, 65S1, 65W1), including GaAs (64B2, 66H1, 66K2). In GaAs the oscillatory frequency has been found to be in the range of $10^5$ Hz for fields over 800 V/cm. As well, it has been found that the oscillatory period is independent of the applied field once the threshold value was reached. While the threshold field found in this work is the same as that needed for the acoustoelectric effect, the free carrier concentration, and thus the $n\ell$ product, (as will be seen), was too small for the effect to occur. In this work, the oscillatory frequency was several orders of magnitude smaller than that due to the acoustoelectric effect, and the frequency-field independence did not appear. The next mechanism, however, yields results consistent with the ones obtained in this research.

### 1.3 - Field Dependent Trapping

The third mechanism that can induce N.D.R. in a material is field dependent trapping (F.D.T.) of free carriers. Generally, the capture cross-section of a charge carrier by an impurity centre in a semiconductor is dependent on the energy of the charge carrier. Now, since an electric field can increase the energy of the charge carriers, the capture cross-section, and thus the rate of capture of the charge carriers, will also depend on the strength of the electric field. Therefore the condition needed for N.D.R. is that the capture rate increase with increasing electric field above a certain critical value of field. This condition could be satisfied if the centres in a particular level presented a modified repulsive Coulomb potential to the charge carriers so that the carriers would

have to surmount a barrier before they would be trapped.

The potential distribution around a repulsive centre is shown schematically in Fig. 2-1. It may be thought of as a superposition of a Coulomb repulsive potential due to electrostatic repulsion and a short range attractive potential. The attractive potential would be due to the impurity atom not having as yet satisfied fully its orbital condition. Once the electron has overcome the net negative repulsive force it sees at large distances, it would be trapped at the centre. $\phi$ in this case is the potential barrier the electron has to overcome to be captured.

At low fields no charge carriers would be trapped, but as the field increased, more and more carriers would have sufficient energy to surmount the barrier and be captured by the impurity centre. Assuming that the lattice temperature remains constant and that no impact ionization occurs, then the generation rate of carriers remains constant for increasing field and a drop in carrier density occurs.

It can be shown (Appendix) that the barrier height $\phi$ for F.D.T. to be effective must be $\phi > 0.08$ eV. Barriers of up to 0.2 eV have been measured for copper, nickel and gold in Ge (55B1, 56S1, 60J1). Ridley and Pratt (65R2) have observed N.D.R. due to F.D.T. of electrons in n-type Ge containing $Au^{--}$ centres.

Current oscillations due to F.D.T. have been observed in high resistivity GaAs by a number of authors (ref. given in Chapter I). The oscillations occur for applied fields of 200 to 2,000 V/cm and have a frequency of $10^{-1}$ to $10^{5}$ Hz which is field dependent. As will be seen in Chapter IV, the experimental results obtained in this work satisfy the

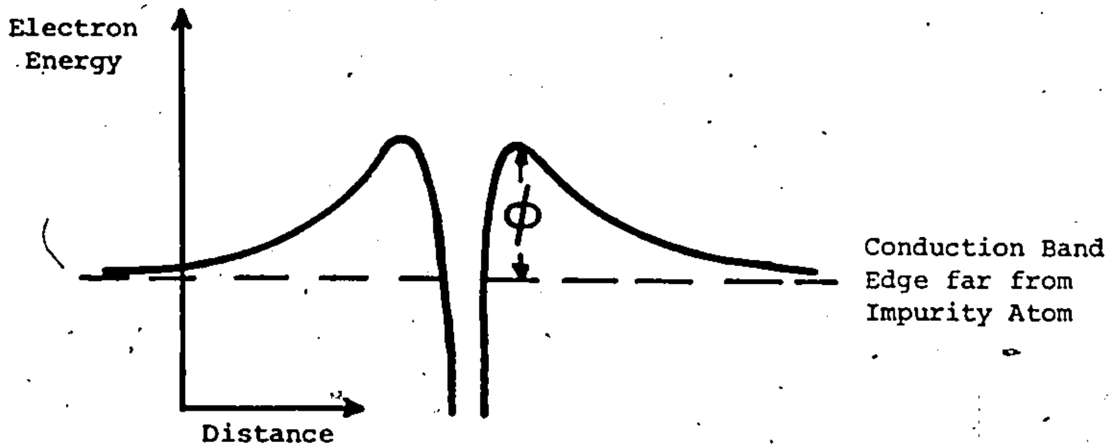


Fig. 2-1 Schematic Diagram of Potential Around A Negatively Charged Impurity Centre.

LIBRARY

above conditions.

The above explanation of the F.D.T. effect is fairly descriptive. For a more detailed analysis, the reader is referred to the Appendix at the end of this manuscript.

### 1.4 - Other Effects

A number of other mechanisms responsible for N.D.R. in a crystal have been suggested. These include: electrons exhibiting negative effective mass at certain high electric fields (59K1); anisotropy and population shifts of the many-valley structure of the conduction band in Ge (63E1); and the field-quenching effect (59B1). Except for the last mechanism, which differs little from F.D.T. (65B4), no experimental evidence has been found to support these theories, and N.D.R. is usually attributed to one of the three mechanisms discussed in the last three sections.

## II-2 High Field Domain

A bulk semiconductor exhibiting differential negative resistance is inherently unstable (63R1). This is because a random fluctuation of carrier density at any point in the semiconductor produces a momentary space charge which grows exponentially in space and time. Of interest here is the bulk negative resistance behaviour of GaAs due to voltage controlled differential negative resistance (the other type is current controlled). The general current density vs. electric field characteristics of such a crystal is shown in Fig. 2-2. As can be seen from this Fig., for voltage controlled N.D.R. the electric field is multivalued. The J-E

VANIER LIBRARY UNIVERSITY OF OTTAWA

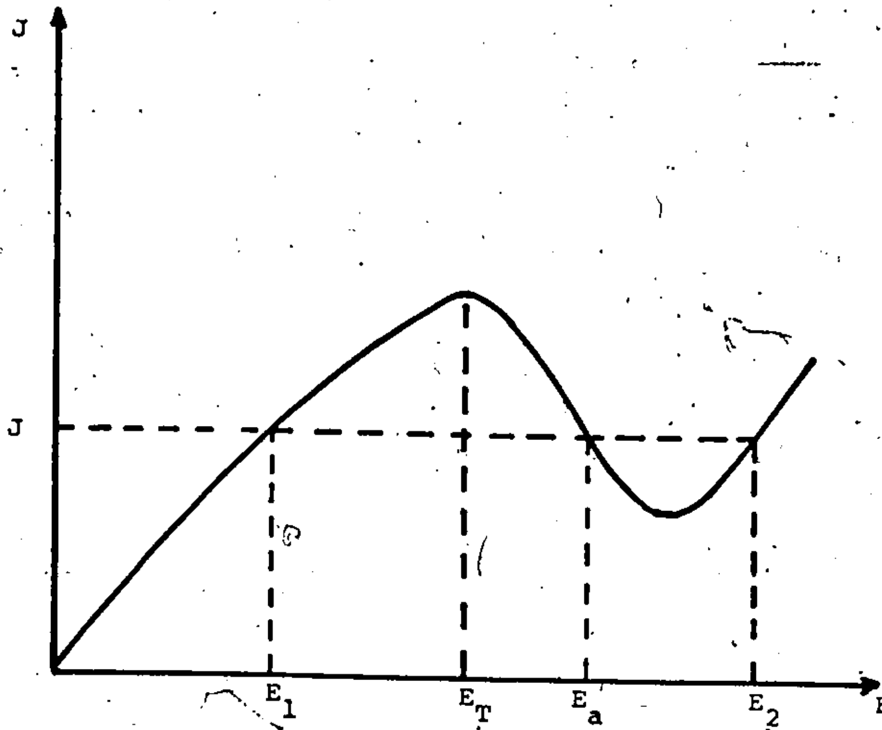


Fig. 2-2 Current-Density (J) vs. Electric Field (E) Characteristics for Voltage Controlled N.D.R.

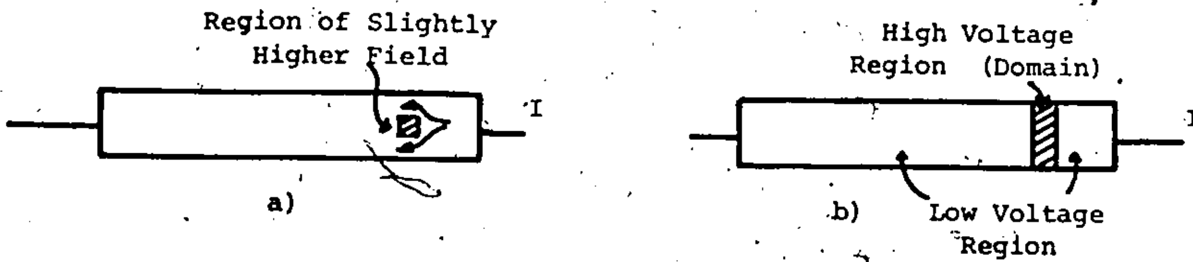


Fig. 2-3 Formation of High-Field Domain in a Voltage Controlled N.D.R.

curve shown in Fig. 2-2 refers to the microscopic instantaneous characteristics of the bulk semiconductor and are not the D.C. characteristics.

Because of the N.D.R., the semiconductor, initially homogeneous, becomes electrically heterogeneous in an attempt to reach stability. For voltage controlled N.D.R., this results in the formation of travelling high field domains. Ridley has shown (63R1) that for voltage controlled N.D.R., the electrical state most favoured by the principle of least entropy production is the one which has least Joule heating, leading to the material splitting up into domains. It can be seen from Fig. 2-2 that the differential positive resistance increases with field, or $\frac{dR}{dE} > 0$. If, however, there is a region of slightly higher field as shown in Fig. 2-3a, the resistance in this region is larger. Thus less current will flow through this region, and in fact the current will tend to flow around it. This will result in the region elongating in a direction perpendicular to that of the current flow to form a high-field domain, which separates the regions of low field as shown in Fig. 2-3b. The interfaces separating low- and high-field domains must lie along equipotentials so that they are in planes perpendicular to the current directions.

One can consider the behaviour of such a crystal in more detail if one considers the crystal to be biased for a field $E_A$ (see Fig. 2-2). At some point A in the crystal there exists a region of high resistivity which could be due to a random noise fluctuation, or possibly a permanent non-uniformity in doping. This means that the field will become non-homogeneous across the sample, or in other words, there will be more carriers flowing into the region than out. If there are two types of

carriers separated by a small distance d, there will be a dipole formation, or domain, created as shown in Fig. 2-4a, resulting from the fact that more charge carriers of both types flow into the region than out. The charge distribution at the steady state is shown in Fig. 2-4b, and the resulting electric field distribution in Fig. 2-4c. d in this case will represent the width of the domain. Because of N.D.R., the current in the low-field region will be greater than in the high-field region. The field will continue to grow towards equilibrium levels outside the N.D.R. region, until it reaches a stable configuration for values $E_1$ and $E_2$ when the current flow in both regions will be the same. (see Fig. 2-2). The dipole is now in a stable configuration. The potential distribution is shown in Fig. 2-4d, and it can be seen that the dipole will now travel through the sample towards the region of low potential, or anode. When this occurs and the domain disappears at the anode, the field will begin to rise uniformly across the sample from its low value $E_1$ until $E > E_T$ ($E_T$ is the threshold field), where a new dipole layer will form at a suitable nucleation centre near the cathode. Thus the process repeats itself.

It has been found that this behaviour is dependent on the product of the number of electrons per cubic centimetre, and the length of the sample ($n\ell$ product) (65Kl, 66Ml). If this product is large (e.g. $n\ell > 10^7$ cm$^{-2}$ for F.D.T.), the dipole layer will grow, and since it is made up of mobile carriers, will travel as it grows. As mentioned, growth continues until the current flow in both regions of the domain equalizes. For this to occur, the number of carriers must be sufficiently large so that the necessary amount of space charge is built up during the transit

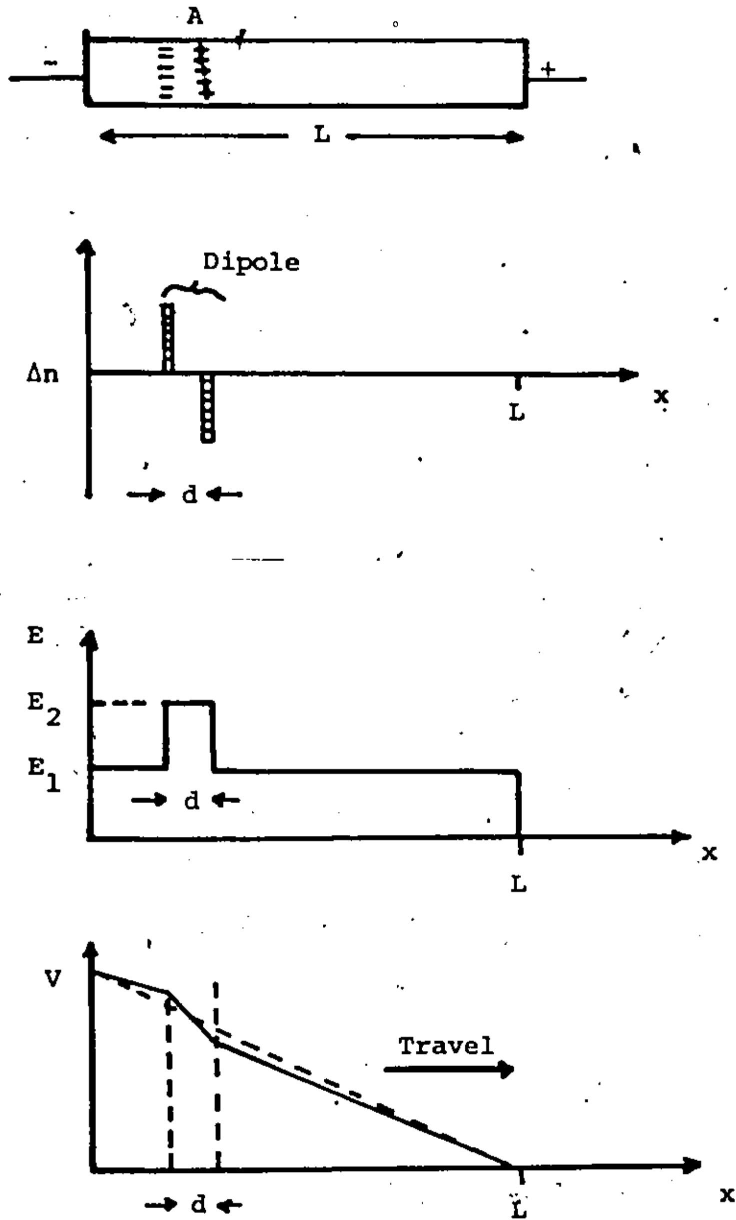


Fig. 2-4 Formation of a Domain in a Perturbed Medium of Negative Resistivity

time of the domain (before it reaches the anode). When the $n\ell$ product is not large enough to produce this behaviour, a steady state occurs in which the field and charges are so redistributed in the sample that the differential resistance as measured across the sample terminals is positive (66M1, 54S1).

Travelling high field domains such as described above have been observed in a number of semiconductors, among them Ge (65R2, 66K2, 67K2) and CdS (59B1, 65B4), as well as GaAs (69S1, 69T2, 67K1, 67T1, 64N1, 70L1). Boer in particular has observed the travelling domains in CdS and photographed them (both still and movie photographs) using the Franz-Keldysh effect (61B3). Similar photographic experiments on GaAs also using the Franz-Keldysh effect were initially unsuccessful (65S2), but more refined techniques and a better choice of illuminating light by Shirafuji (68S1), succeeded in obtaining photographs of the travelling domains in semi-insulating neutron irradiated GaAs.

In very high resistivity samples at low temperatures, the need for a sufficiently high $n\ell$ product to obtain the travelling domains may require the optical generation of free carriers. Even then, in some cases, optical excitation across the gap would not increase the free carrier concentration sufficiently for domain formation were it not for the presence of certain centres in the material (sensitizing centres) which greatly enhance the photoconductivity. Since this behaviour was present in the sample used in this study, the next section will describe this "sensitization of photocurrent" effect.

## II-3 Optical Sensitizing Centres

Consider a semiconductor containing two impurity levels in the forbidden gap, as illustrated in Fig. 2-5a. The s centres (fast centres), with approximately equal capture cross section for electrons and holes, will normally be located just below the conduction band and will act as recombination centres, while the r centres (slow centres), with much larger cross sections for the capture of free holes than they have subsequently for the capture of free electrons, will be above the valence band and thus be hole traps. Such r centres have been reported for GaAs by a number of authors (72B2, 69S1, 67S1).

According to Bube, under optical excitation of such a material with intrinsic light, the Fermi level for thermal equilibrium is replaced by an electron Fermi level ($E_{fn}$) and a hole demarcation level ($E_{dp}$), (60B1) as illustrated in Fig. 2-5b . These two levels divide the gap into regions of traps and recombination centres as follows. If a hole is located at the hole demarcation level, it has equal probability of recombining with a free electron and of being thermally ejected to the valence band. Thus all centres lying between the electron Fermi level and hole demarcation level act as recombination centres; all centres lying above $E_{fn}$ are electron traps; and all centres lying below $E_{dp}$ are hole traps.

Consider the effect these levels will have at low temperature on a high resistivity material where the density of carriers under optical excitation is much larger than the thermal generation of carriers. If there is only one type of centre between $E_{fn}$ and $E_{dp}$, with about equal capture cross section for holes and electrons, then this level will act as

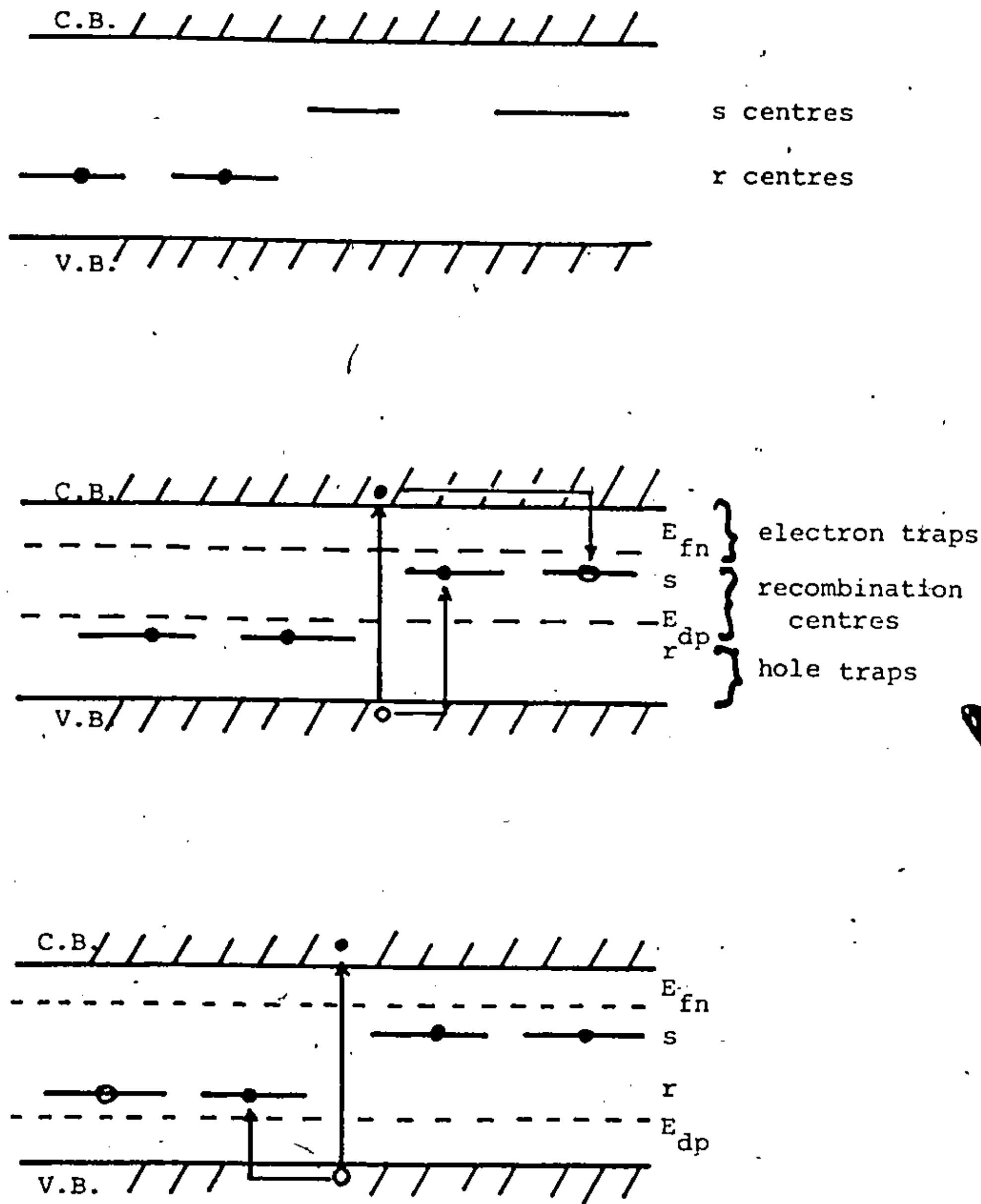


Fig. 2-5 Excitation and Recombination Processes in a Photoconductor with Fast and Slow Recombination Centres.

VANIER LI

a recombination level and will produce a small free lifetime for photo-excited carriers. The r centres, if they are compensated acceptors and thus contain an extra electron, have little effect on the sensitivity of the material since they lie below the hole demarcation level (Fig. 2-5b). If however the temperature is decreased (or the light intensity increased), the hole demarcation level shifts to below the r centres (62B2) and the material becomes sensitized for the following reason: both r and s centres now act as recombination centres. Holes captured at r centres have a longer life there before recombination than holes captured at s centres. Thus the r centres become occupied principally by holes, or in effect, most of the electrons in the r centres become effectively transferred to the s centres. Thus the lifetime of the free electron is increased since it faces mainly centres with small capture cross sections (r centres) and almost no centres with large capture cross section (s centres). The result of this process is thus an increase in photoconductivity as the temperature of the sample is lowered. References to sensitizing centres found in GaAs (as well as other materials), with further elaboration into the effect, will be given when the results are discussed in Chapter IV.

# CHAPTER III EXPERIMENTAL MATERIAL, EQUIPMENT AND PROCEDURE

## III-1 Material and Equipment

### 1.1 - Some Properties of Gallium Arsenide

Gallium Arsenide is a heteropolar III-V semiconductor with a band gap of 1.43 eV at 300°K. It thus occupies a position intermediate between the lower band gap group IV elemental semiconductors (e.g. Ge and Si) and the higher band gap II-VI photoconductors (e.g. CdS)(61B1). Because of its fairly large band gap, very pure GaAs would act as an insulator, but in practice it is found that it is very difficult to keep the material pure when preparing it. As a result of this, standard preparation of this compound (ingots grown by a conventional Bridgman technique (59W1)) yields monocrystalline n-type GaAs with electron concentrations in the order of $10^{16}$ - $10^{17}$ $cm^{-3}$, and electron mobilities varying from 2,700 to 5,600 $cm^2V^{-1}sec^{-1}$ at 300°K (61B1). The relatively low resistivity of the material ( $< 10^3\Omega$-cm) is due to the inadvertent introduction of impurities in the material during preparation, no matter how carefully the preparation is done. The result is a multitude of impurity levels in the material, with some of these now known, but with many more still being investigated.

The standard procedure for obtaining high resistivity GaAs is to compensate normal low resistivity material. A number of compensating methods have been used ranging from direct evaporation of copper and then annealing (61B1) to neutron irradiation of the material (69S1). The objective, though, is the same: to compensate shallow donor levels (or acceptor levels if p-type GaAs is initially obtained) and so increase the

energy difference existing between the conduction band and the first (or nearest) impurity level containing electrons. This method is quite effective and semi-insulating GaAs with resistivities of the order of $10^8 - 10^9\ \Omega$-cm at $300^\circ$K is now commercially available.

One of the characteristics that makes GaAs an interesting material to study is the fact that its conduction band has a subsidiary minimum along the [100] direction in k-space, and the energy difference between two of them is quite large, in the order of 0.35eV(69V3). In semi-insulating GaAs it is possible to apply a sufficiently high electric field to "heat" some of the carriers in the lower minima and have them transfer to the higher one. Since the upper valley has a much larger effective mass, the current drops for increased applied electric field and N.D.R. (and resulting Gunn oscillations) set in, as described in the last Chapter. However, as was also discussed in the last Chapter, there are other N.D.R. mechanisms that can induce current oscillations .

1.2 - Sample Preparation

The monocrystal <111> Cr compensated high-resistivity ($\rho > 10^7\ \Omega$-cm) GaAs slab was obtained commercially from Monsanto (St.Louis), and was cut into parallelepipeds of dimensions approximately 10 x 2 x 0.5 $mm^3$. The sample was first glued to an adjustable lapping holder by means of glyptol thinned with acetone, and all six sides were lapped using 5μ alumina powder moistened with distilled water.

The specimen was then chemically polished for two minutes at $70^\circ$C in a solution of $HNO_3$:HF:$H_2O$ in a 3:1:2 ratio.

After the surface treatment, Indium wire of 99.999% purity was evaporated onto the ends of the sample to serve as contacts located about 5 mm apart. This was performed under a vacuum of $10^{-6}$ mm Hg in a Veeco-400 Evaporator. The contacts were then annealed in a Helium atmosphere at 450°C for three minutes. The end contacts resulting were ohmic.

Specimen dimensions were measured by means of a Vernier microscope which had an accuracy of $\pm 1 \times 10^{-2}$ mm. Fig. 3-1 shows a typical sample with In contacts evaporated on.

### 1.3 - General Apparatus

The principal piece of apparatus used in the experiments was an OPTICAL CRYOSTAT (70F1) made of stainless steel and brass, with the lower portion of the cryostat having a detachable tail-piece fitted with a quartz window. At liquid nitrogen temperatures a vacuum of the order of $10^{-6}$ mm Hg could be obtained. Fig. 3-2 shows a cross-sectional diagram of the cryostat.

The inner tail assembly had a BeO plate fixed to it allowing very high electrical insulation and good thermal contact. The temperature was measured using a copper constantan thermocouple affixed to the rear face of the BeO plate, with the E.M.F. being monitored by a Hewlett-Packard 3440 A Digital Voltmeter. The specimen was mounted on the front face of the BeO plate using copper pressure contacts.

The voltage applied to the specimen was supplied by a Keithley 240 A High Voltage Supply for the high field runs, and a standard 1.32 volt Hg cell for the low voltage measurements. Both power supplies were monitored

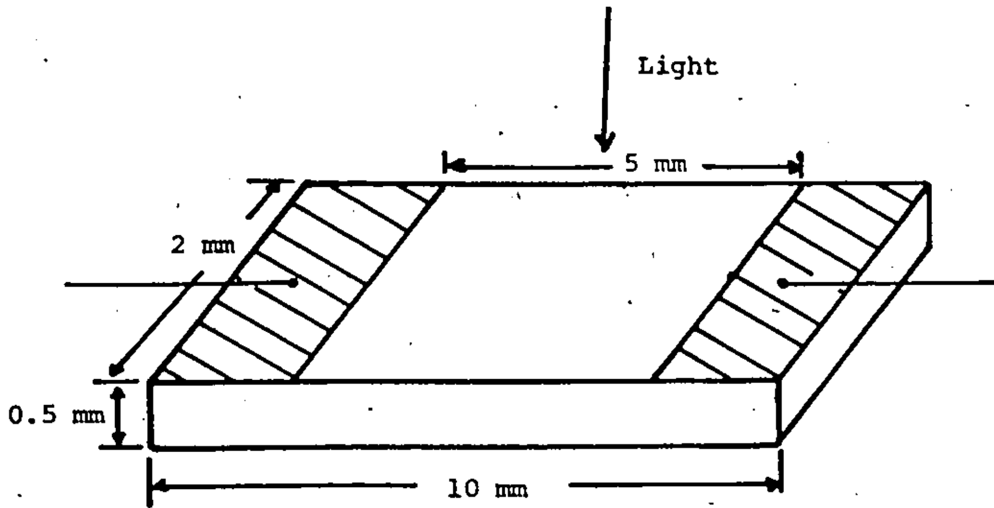


Fig. 3-1 GaAs Sample with Indium Contacts

Fig. 3-2 Cross-section of Optical Cryostat

a) Cross-section of Optical Cryostat (rear view)

b) Cross-section of optical Cryostat (front view)

c) Detail of Removable Radiation Shield

VANIER LI

a)

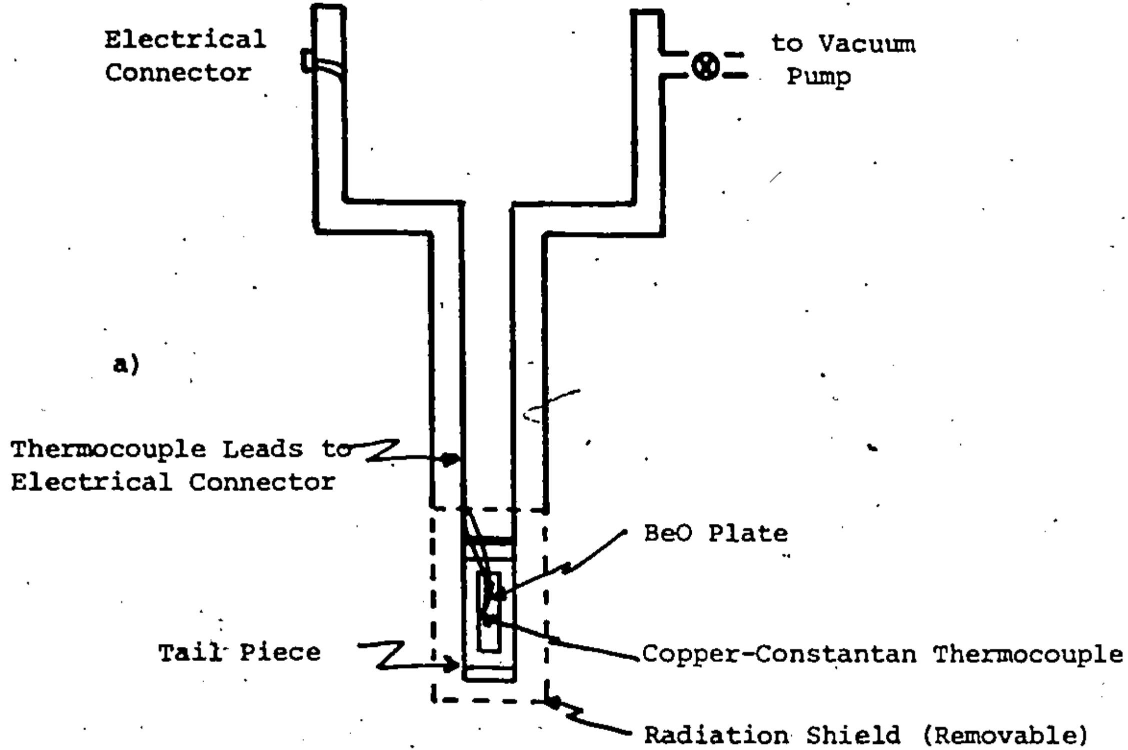


b)

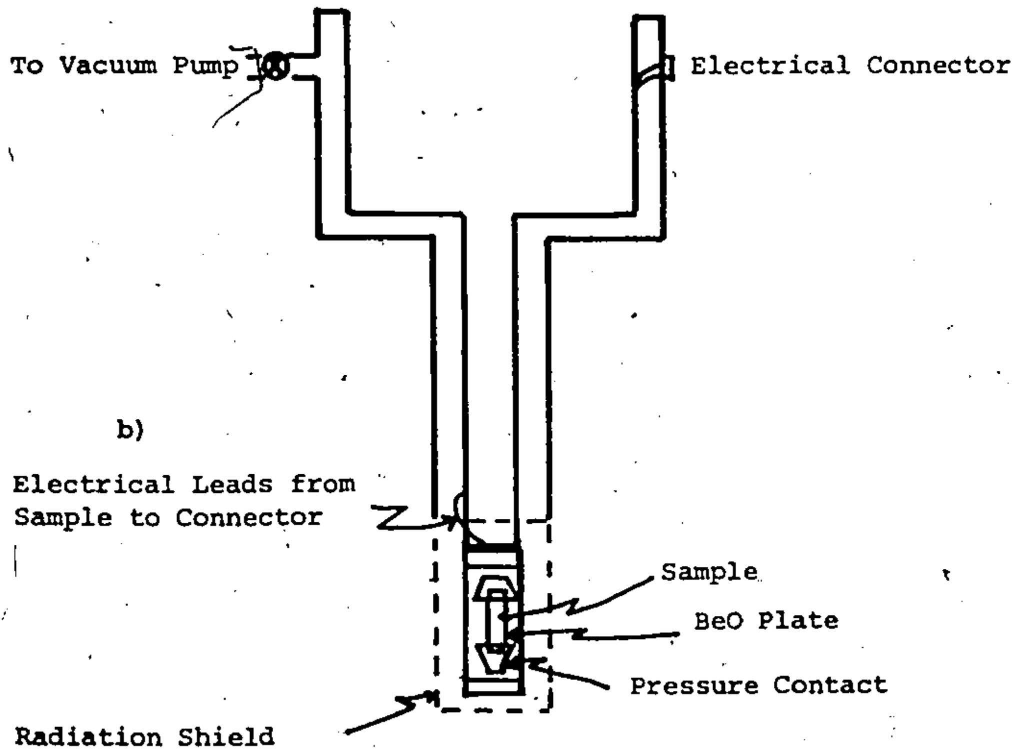


c)

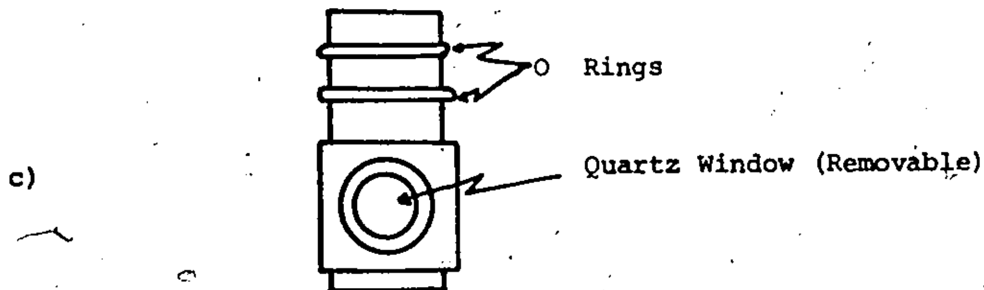

using a Selectest "Super 50" voltmeter. The signal from the sample was monitored using a Keithley Model 602 Solid State Electrometer whose input resistance was greater than $10^{14}\Omega$. When current oscillations were present, their waveform was observed on a Tetronix 545 B Oscilloscope fed from the electrometer, while the oscillatory frequency was measured on a General Radio 1192/Z Counter via the same electrometer. Fig. 3.3 shows a schematic block diagram of the apparatus.

Monochromatic radiation was obtained from a Bausch and Lomb High Intensity Grating Monochromator fitted with the appropriate Kodak filters so as to cut out the $2^{nd}$ and higher order radiation. The output of the monochromator was calibrated using an Eppley vacuum-type thermopile connected to a KIPP and ZONEN high sensitivity "Microva" Multirange Microammeter. The Entrance slit was kept at either 3.56 or 1.78 mm, while the Exit slit was 2.00 or 1.00 mm, and the spectral range scanned was between $0.7\mu$ and $1.6\mu$. A black opaque tube was connected directly from the exit slit to the quartz window of the cryostat to eliminate external radiation, as illustrated in Fig. 3-4.

In the optical quenching experiments, excitation radiation was provided by a quartz-iodide source in association with a $0.90\mu$ interference filter, while the Bausch and Lomb monochromator was used as the quenching source. The electrical connections to the specimen were the same as in the first part, except that the oscilloscope used was a Tetronix 502 A Dual Beam Oscilloscope and the frequency counter was replaced by a Honeywell Electronik 19 Chart Recorder which allowed a permanent record of the oscillations to be obtained. Fig. 3-5 shows the optical arrangement for

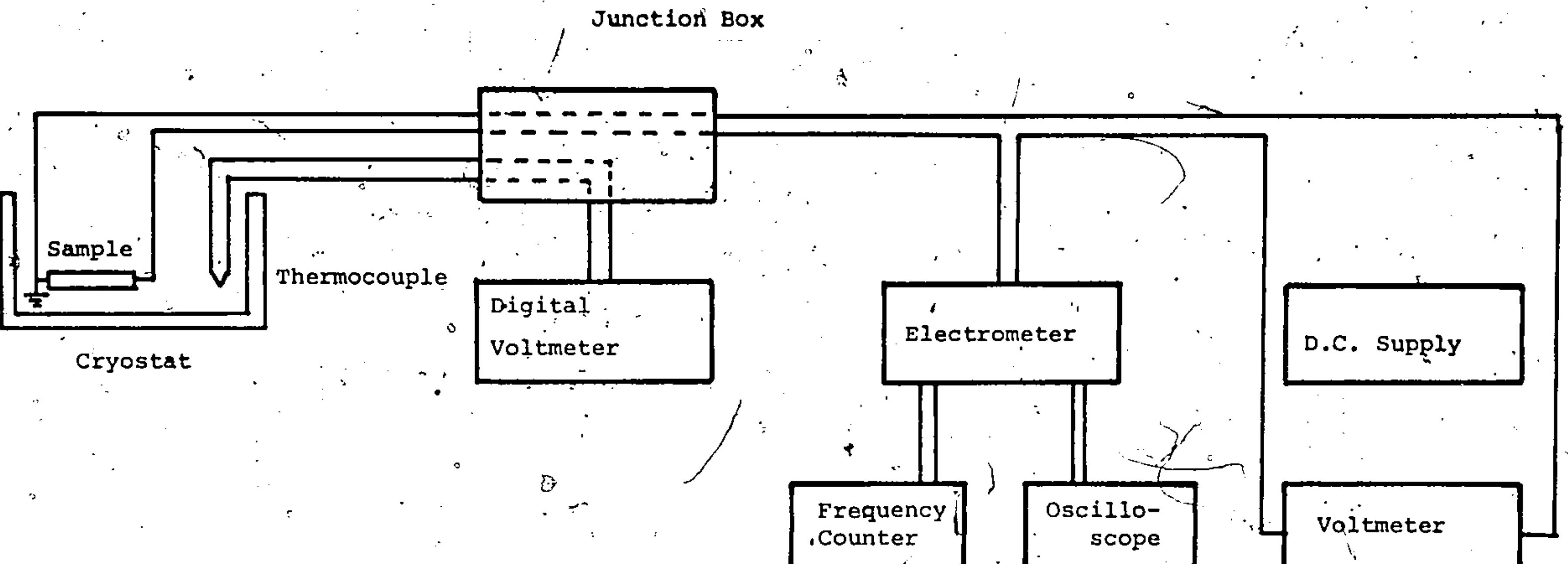


Fig. 3-3 Schematic Block Diagram of Apparatus

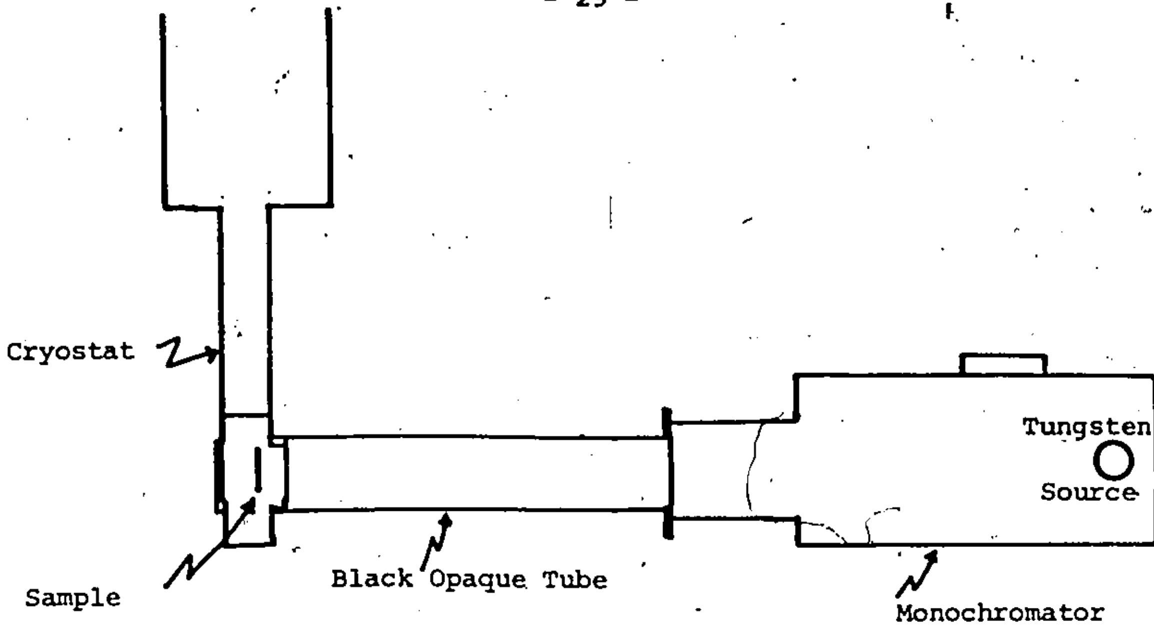


Fig. 3-4 Experimental Arrangement - Single Source

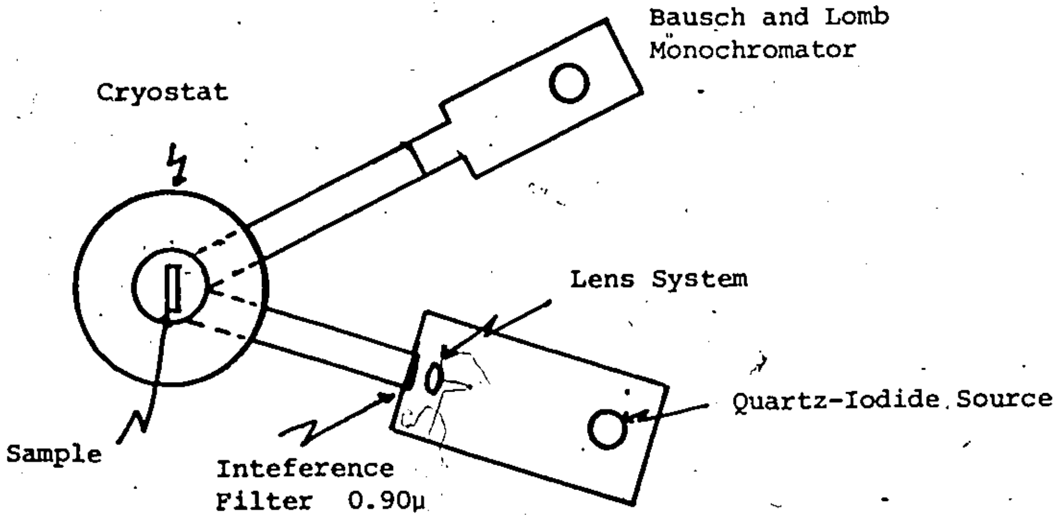


Fig. 3-5 Experimental Arrangement - Double Source

VANIER L

the two source experiments.

The quenching experiments were repeated using the Bausch and Lomb monochromator as the exciting source and a Spex 3/4 metre Czerny Turner Spectrometer as the quenching source (in conjunction with the appropriate Corning and OCLI filters). The Spex spectrometer had a motorized adjustable scan rate and allowed the spectral range from 0.65μ to 2.05μ to be investigated.

## III-2 Procedure

The study of the GaAs was divided into two main areas:

1 - Electrical and Optical Properties

2 - Current Oscillations and Quenching.

Initially measurements were made at both 300°K and 90°K but this procedure was discontinued when the 90°K measurements proved the more interesting and fruitful.

### 2.1 - Electrical and Optical Properties

#### 2.1.1 I-V Characteristics

The dark current $I_d$ was measured as a function of applied voltage V at 90°K, the lowest temperature that could be consistently reached with the cryostat, and at 300°K, room temperature. The aim here was to see if it was possible to detect any negative resistance characteristics in the sample, as well as to determine the ohmic region for the specimen. The procedure was then repeated for the photocurrent $I_p$ for an excitation radiation of 0.90μ (approximately band gap value at 300°K).

At $300^{\circ}K$ the dark current was always subtracted from the measured photocurrent to obtain the true photocurrent, but at $90^{\circ}K$ the measured value of photocurrent was used since the dark current was negligible. For example, for V = 400 volts at $300^{\circ}K$, $I_d \sim 0.7\mu A$, while $I_p \sim 9.0\mu A$ for an excitation radiation of 0.90μ. At $90^{\circ}K$, the corresponding currents were $1 \times 10^{-9}$ amps and $8 \times 10^{-5}$ amps respectively.

### 2.1.2 Temperature Dependence of the Current

Since the temperature dependence of the current can yield information on the impurity levels in a material, the dark current of the sample for both low (2.7 V/cm) and high (800 V/cm) field conditions was measured for the temperature range $90^{\circ}K$ to $300^{\circ}K$. As well, the photocurrent of the sample was similarly measured for excitation radiation of wavelengths 0.90μ, 1.16μ and 1.30μ, since these wavelengths were found to have a critical effect on the generation and quenching of the current oscillations.

### 2.1.3 Spectral Response Curves

The photocurrent was measured for wavelengths 0.70μ to 1.60μ (limit of Bausch and Lomb grating) at $300^{\circ}K$ and $90^{\circ}K$, both for low and high field conditions. Since the monochromator had been previously calibrated (see Fig. 3-6 and 3-7) for these spectral regions, a normalized spectral distribution of the current was plotted in all cases.

Fig. 3-6 Calibration Curve For Bausch and Lomb
Monochromator A

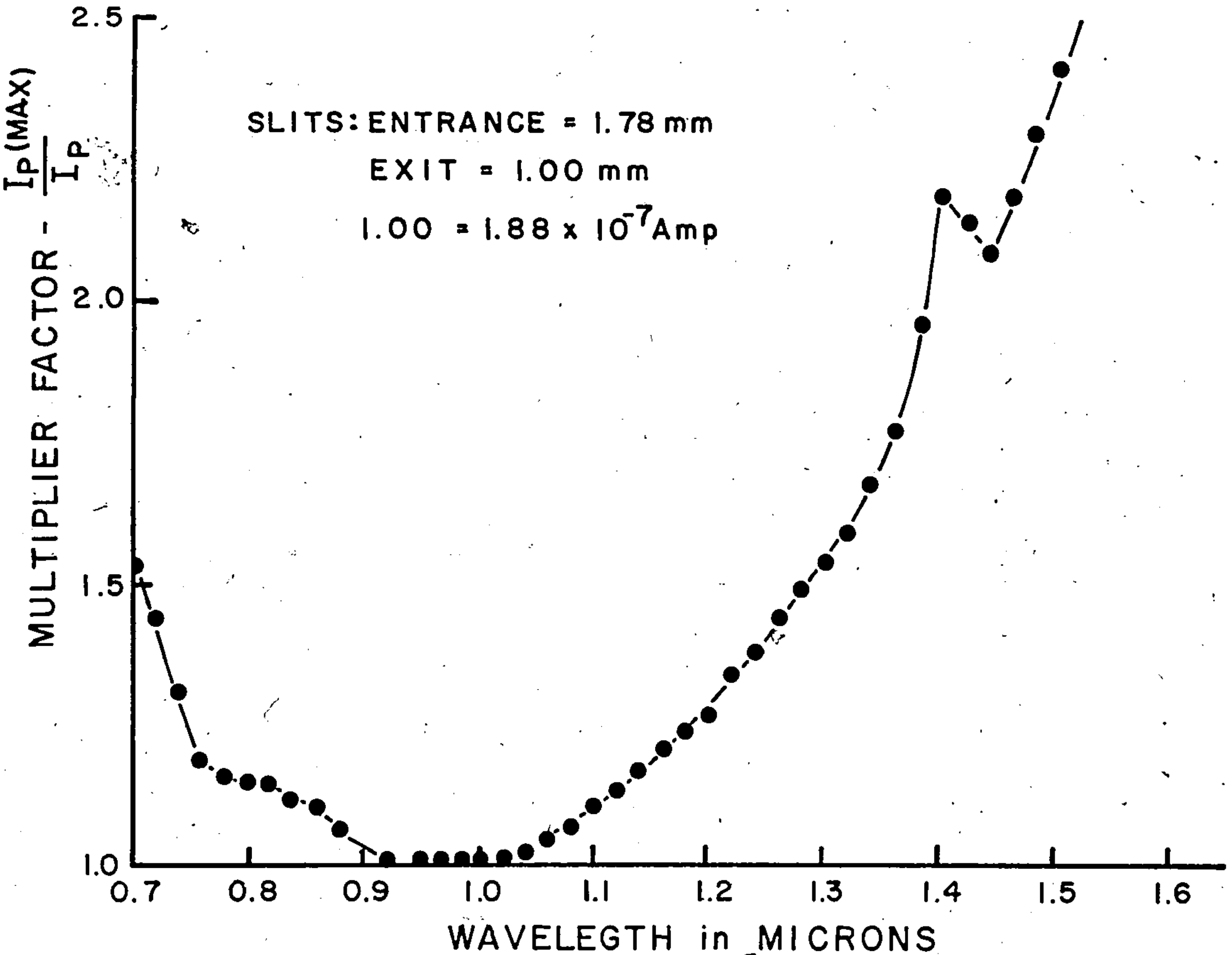
SLITS: ENTRANCE = 1.78 mm
EXIT = 1.00 mm
1.00 = 1.88 x 10$^{-7}$ Amp
MULTIPLIER FACTOR - $\frac{I_p(MAX)}{I_p}$
2.5
2.0
1.5
1.0
0.7
0.8
0.9
1.0
1.1
1.2
1.3
1.4
1.5
1.6
WAVELEGTH in MICRONS

Fig. 3-7 Calibration Curve for Bausch and Lomb Monochromator B

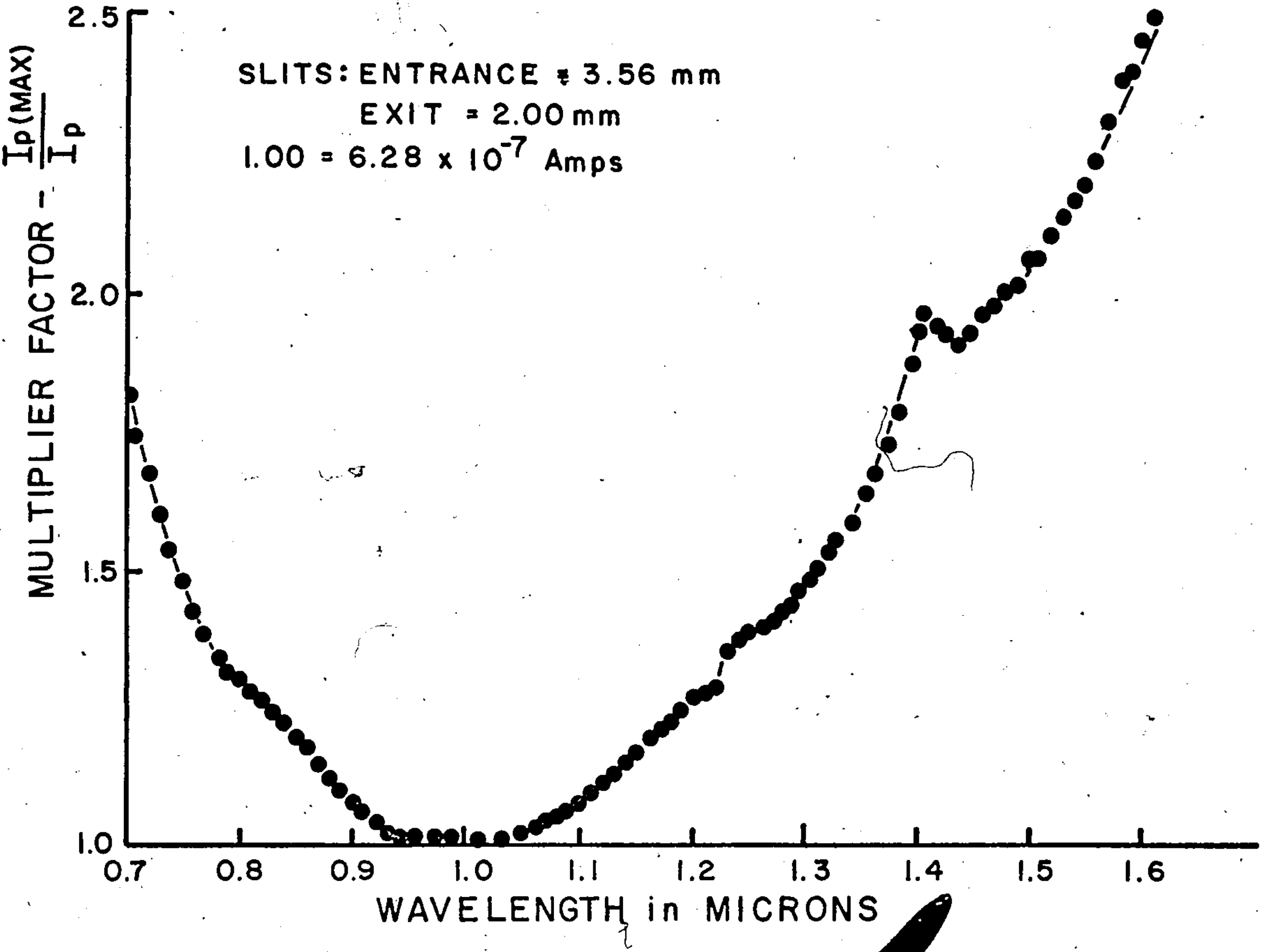
SLITS: ENTRANCE = 3.56 mm
EXIT = 2.00 mm
1.00 = 6.28 x 10^-7 Amps
MULTIPLIER FACTOR - Ip(MAX)/Ip
2.5
2.0
1.5
1.0
0.7
0.8
0.9
1.0
1.1
1.2
1.3
1.4
1.5
1.6
WAVELENGTH in MICRONS

## 2.2 - Current Oscillations and Quenching

### 2.2.1 Dependence of Frequency of Current Oscillations on:

A. Temperature: as it was found that the photocurrent oscillations for a fixed applied field would appear only below certain temperatures, the dependence of the frequency of oscillations of the photocurrent on the temperature was investigated for an applied field of 800 V/cm and an exciting radiation of 0.90μ. The procedure was to quickly cool the specimen in the dark with liquid nitrogen from 300°K down to about 90°K. The 0.90μ radiation was then used to generate the oscillations and while monitoring the frequency of the oscillations, the sample was allowed to heat up to 300°K over a period of two or three hours. It was not possible to reverse the procedure since the cooling rate could not then be controlled.

B. Intensity: because the intensity of the exciting radiation had a bearing on the generation of photocarriers, its effect on the frequency of oscillations was measured at 90°K and 800 V/cm for 0.90μ radiation by adjusting the size of the entrance slit of the monochromator while keeping the exit slit fixed. The intensity calibration for the monochromator at 0.90μ is given in Fig. 3-8.

C. Wavelength: at low temperature the oscillations were present only when the sample was irradiated with infrared of certain wavelengths, so the behaviour of the oscillations as a function of exciting wavelength, again at 90°K and 800 V/cm, was measured.

D. Voltage: the voltage applied to the sample was a critical factor in generating oscillations, so its effect on the frequency at 300°K was measured. As well, this allowed the determination of the minimum

Fig. 3-8 Intensity Calibration

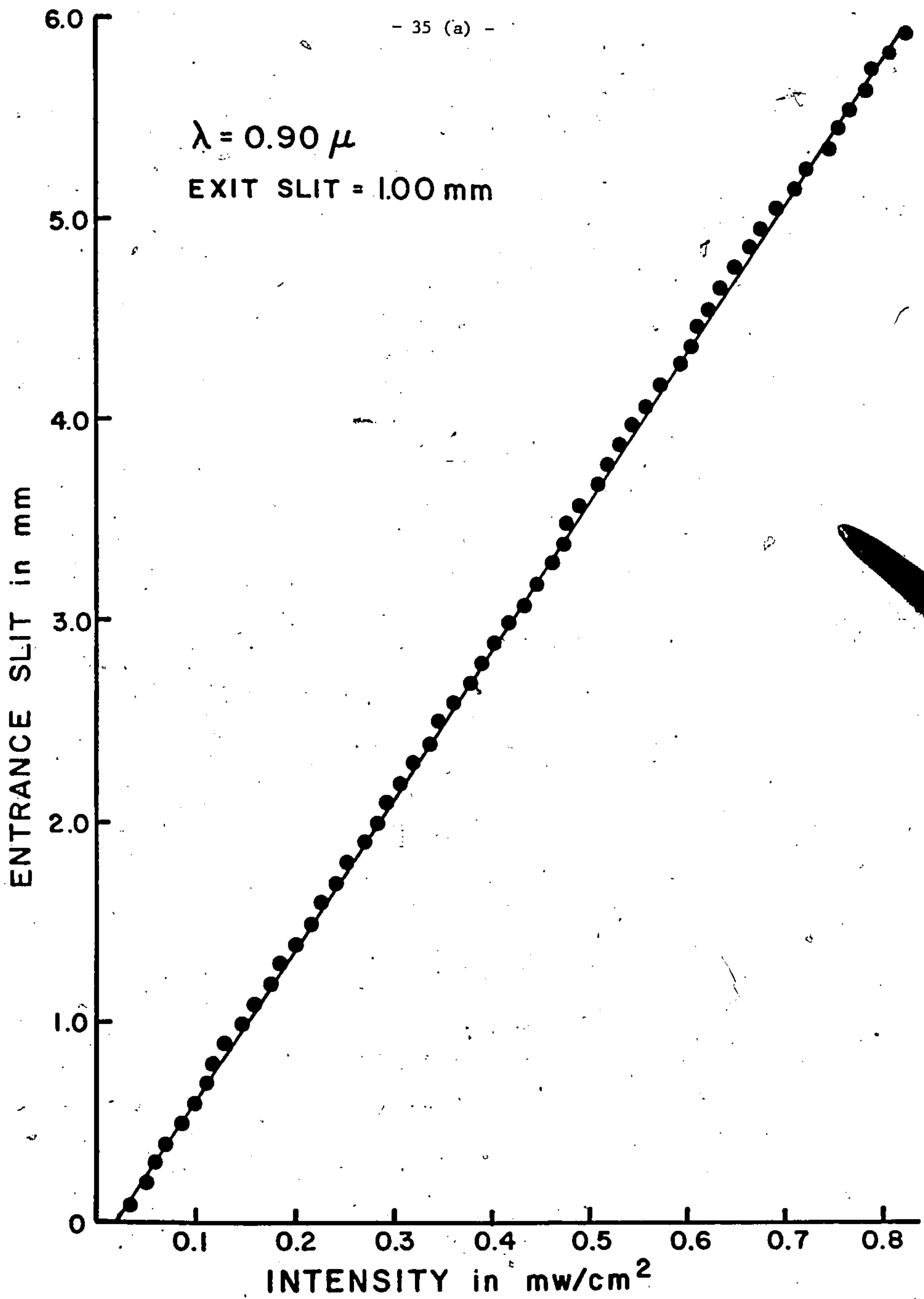
λ = 0.90 μ
EXIT SLIT = 1.00 mm
ENTRANCE SLIT in mm
INTENSITY in mw/cm²
6.0
5.0
4.0
3.0
2.0
1.0
0
0.1
0.2
0.3
0.4
0.5
0.6
0.7
0.8

voltage required for oscillations

2.2.2 Quenching:

A. Thermal: thermal quenching of the oscillations was determined from the temperature dependence of the high field photocurrent, as outlined in section 2.2.1A.

B. Optical: the investigation of the self-quenching of the oscillations as the wavelength of the exciting radiation was varied was performed by analysis of the spectral response curves measured in section 2.1.3.

C. Second Source: the two source experiment allowed a determination of the wavelengths at which a second optical source could quench the oscillations being generated by a primary source. The specimen was cooled down to 90°K and then an 800 V/cm field and 0.90μ radiation was applied to it. This procedure would generate the oscillations. The second source would be used to scan up in energy from about 2.0μ until the oscillations were quenched. After the oscillations were regenerated by warming the specimen above ∿ 125°K and recooling to 90°K, the procedure was repeated, but this time by scanning down in energy from 0.7μ. This allowed a determination of the range of wavelengths over which the quenching was effective. To determine any intermediary values of wavelength which would not quench the oscillations, the automatic scanning would be started on a new run at a certain wavelength past the quenching wavelength, again from both high energy and low energy values. By this method it was possible to determine over which ranges of wavelength (and hence energy) the oscillations were

optically quenched.

The results obtained by following the procedures outlined in this Chapter are given and discussed in the following Chapter.

# CHAPTER IV RESULTS AND DISCUSSION

The experimental results obtained by following the procedures described in the previous Chapter, and the interpretation of these results, are discussed in this Chapter under three main headings:

1 - Electrical Properties,

2 - Optical Properties,

3 - Current Oscillations and Quenching.

A number of parameters pertinent to the oscillations are calculated from these results. As well, the energy values of some of the impurity levels in GaAs are evaluated, in particular those levels responsible for F.D.T. and the quenching of the oscillations. These values are then used to discuss the behaviour of the GaAs in terms of an impurity level energy diagram.

## IV-1 Electrical Properties

### 1.1 I-V at 300°K

Previous Hall measurements on the specimens (69M1) have yielded a negative Hall constant at 300°K, while P.E.M.* experiments on the samples indicated that electrons are the minority carriers. It is believed that the GaAs is closely compensated and at temperatures below 300°K dark conductivity is due primarily to holes with the transitions to electron conductivity occurring below, but near 300°K (61B1).

In the dark at 300°K, the specimen was found to exhibit Ohmic behaviour for applied fields of up to 500 V/cm with the resistivity of the

* Photoelectromagnetic

VANIER LIBRARY

sample being about $5 \times 10^8$ Ω-cm (Fig. 4-1). For fields larger than 500 V/cm, the current deviated from Ohm's Law, and in the range of 500 V/cm to 1,800 V/cm (the highest value of field measured), the I-V slope decreased, as illustrated in Fig. 4-1. This behaviour suggests that above the Ohmic region some sort of extraction mechanism is taking free charge carriers out of the conduction process, and that this carrier extraction process increases with field. One possible mechanism would be F.D.T. This possibility is further enhanced by the appearance of current oscillations above an applied field of 950 V/cm. During the oscillations, whose frequency varied between 5 and 10 Hz, the current value would change by about 25%.

Because of the mixed conductivity of the sample at 300°K, it was not possible to obtain the minimum carrier concentration necessary for the onset of current oscillations at 300°K (the minimum $n\ell$ product necessary for domain formation). This is due to the fact that the F.D.T. mechanism is operative on the negative charge carriers (electrons) while the current value at the onset of oscillations is due to both types of carriers (mixed conduction; see 72P4). However, the carrier concentration can be estimated to within an order of magnitude if it is assumed that the current is due primarily to electrons and that the scattering factor is unity, so that $\mu_H = \mu_n$ ($\mu_H$ - Hall mobility, $\mu_n$ - electron mobility). Then, using $\mu_n = -2.3 \times 10^3$ cm$^2$ (V sec)$^{-1}$ (69M2), for a current of $2.1 \times 10^{-7}$ A and a threshold field of $9.5 \times 10^2$ V/cm, the carrier concentration is $9 \times 10^7$ cm$^{-3}$, or approximately $10^8$ cm$^{-3}$. This makes the $n\ell$ product (sample length - 0.50 cm) approximately $5 \times 10^7$ cm$^{-2}$ or roughly $10^7 \sim 10^8$ cm$^{-2}$, in good agreement with reported values for F.D.T. (69S1, 72T1).

Fig. 4-1 I-V Characteristics at $300^{\circ}K$

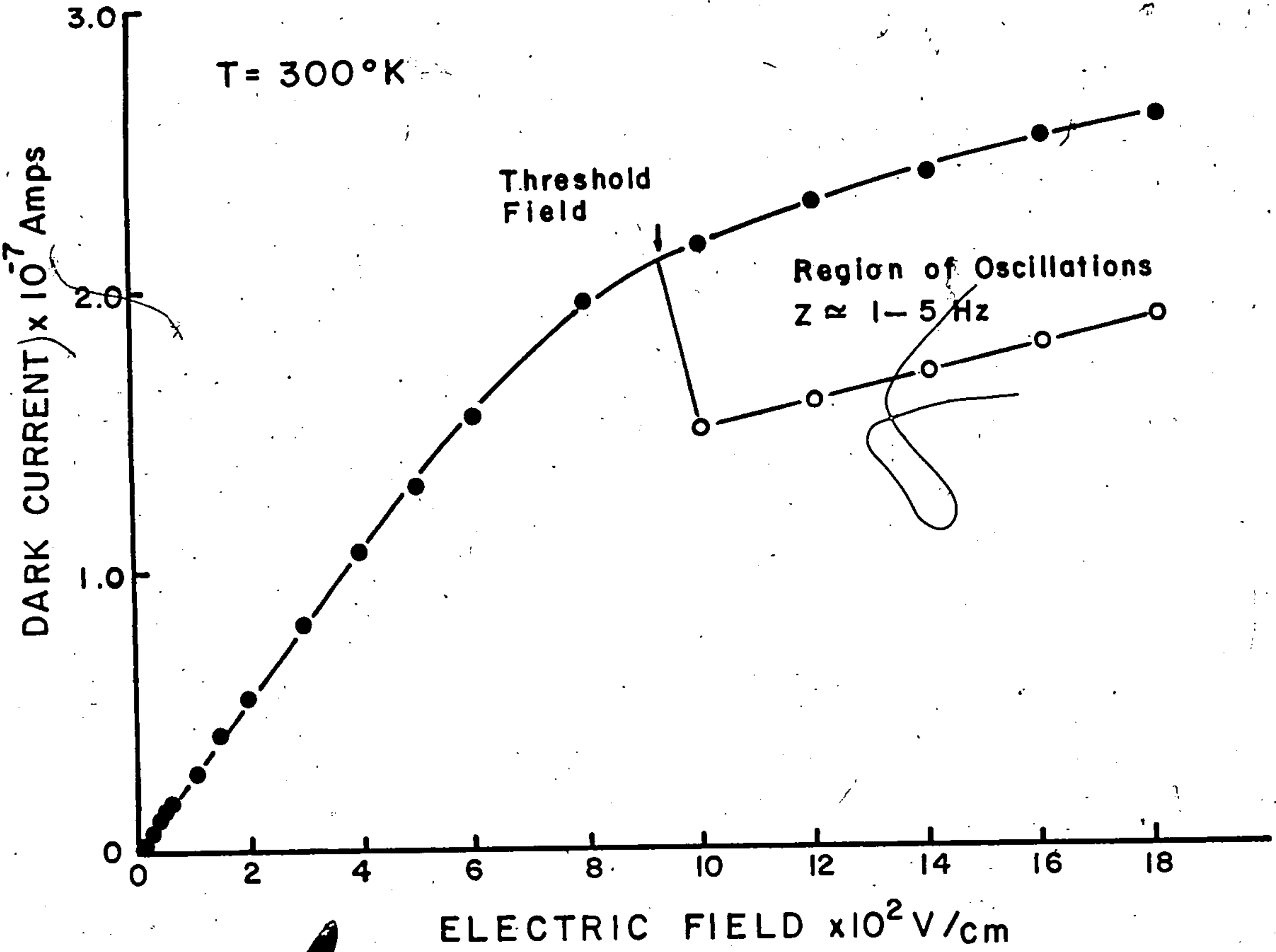
T = 300°K
Threshold
Field
Region of Oscillations
Z ≃ 1—5 Hz
DARK CURRENT x 10$^{-7}$ Amps
ELECTRIC FIELD x10$^2$ V/cm
3.0
2.0
1.0
0
0
2
4
6
8
10
12
14
16
18

Fig. 4-1 has the same characteristics as those reported by other authors for oscillations due to F.D.T. at 300°K (69S1, 69V1, 69V2 72T1).

Because of irregularities in the frequency, as well as the lack of optical data at 300°K, the oscillations were studied primarily at 90°K.

1.2 I-V at 90°K

While it is possible to obtain information about the type of carrier and conduction of semi-insulating GaAs at 300°K in the dark (61B1, 69M1), this information is presently not available for low temperatures (90°K). The reason for this is the increase in the resistivity of the GaAs at the lower temperature, the increase being about four orders of magnitude. As can be seen in Fig. 4-2, for the ohmic region which extends to $10^3$ V/cm, the resistivity of the sample is of the order of $10^{12}$ Ω-cm. For low applied fields (1 ∿ 10 V/cm), the current in the sample is of the order of $10^{-13}$ A, sufficiently close to the limits of the test equipment to make Hall measurements totally inaccurate.

However, as has already been mentioned, below but near 300°K the dark conductivity is due primarily to mobile holes (61B1). Thus, at 90°K one would expect few free electrons contributing to conductivity, and certainly too few to allow for the current oscillations ($n\ell$ product well below minimum required for domain formations), even for fields up to $2 \times 10^3$ V/cm.

If one considers again Fig. 4-2, it can be seen that above $10^3$ V/cm the current deviates from Ohm's Law, but unlike the case at 300°K, the current behaviour is now superlinear. No explanation is known for

Fig. 4-2 I-V Characteristics at 90$^{\circ}$K

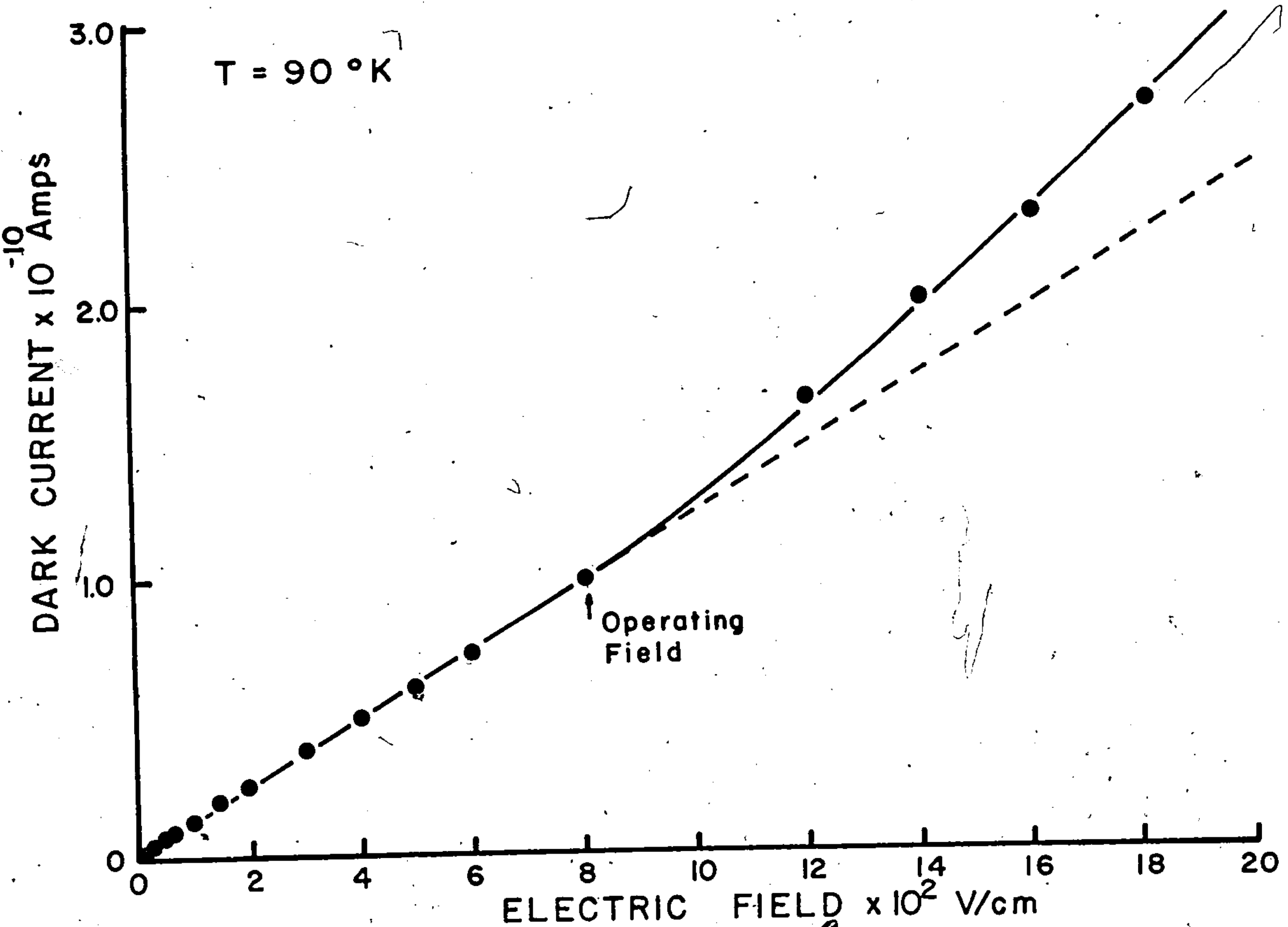
T = 90 °K
DARK CURRENT x $10^{-10}$ Amps
3.0
2.0
1.0
0
ELECTRIC FIELD x $10^2$ V/cm
0
2
4
6
8
10
12
14
16
18
20
Operating Field

Fig. 4-3 Dark Current as a Function of Temperature Under Low and High Field Conditions

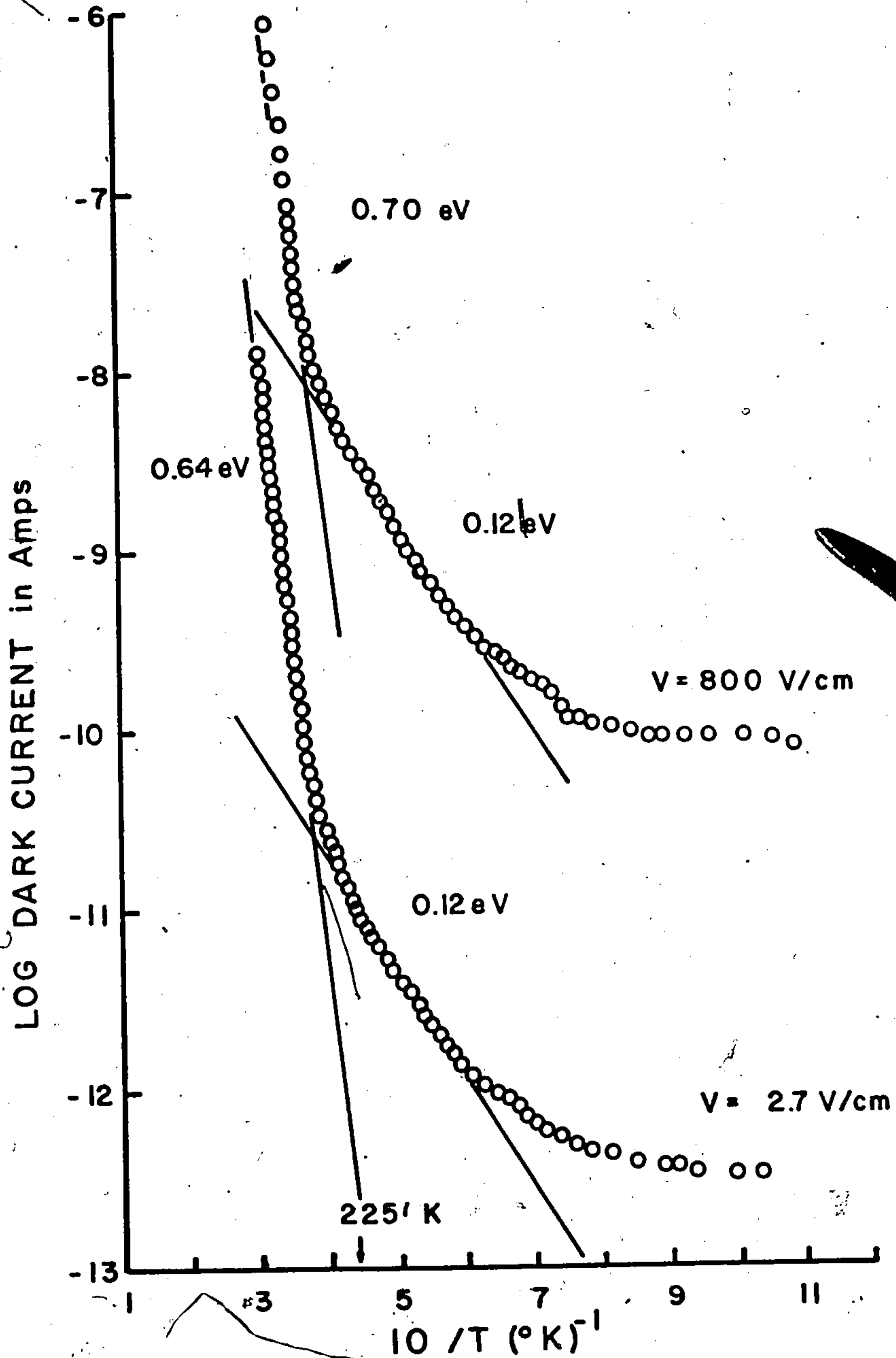
LOG DARK CURRENT in Amps
-6
-7
-8
-9
-10
-11
-12
-13
0.70 eV
0.64 eV
0.12 eV
V = 800 V/cm
0.12 eV
V = 2.7 V/cm
225° K
1
3
5
7
9
11
10 /T (°K)^-1

this behaviour. All measurements were performed below this superlinear region.

1.3 Variation of Dark Current with Temperature

In the lower temperature range of the dark current vs. temperature data (Fig. 4-3), the activation energy obtained from the linear portion of the graph, 0.12 eV, is the same for both low (2.7 V/cm) and high (800 V/cm) field conditions. This is not the case in the higher temperature range (near 300°K), where the activation energies were 0.64 eV and 0.70 eV for low and high fields respectively. The reason for this discrepancy is probably due to the following factor: at lower temperatures both values of field used were in the ohmic region of the sample. At higher temperatures, however, the high field value falls in the non-ohmic region and therefore different conditions are operative. Consider the higher temperature region first.

As has been mentioned, it is believed that below 300°K the dark conductivity is due primarily to holes. In that case, the 0.64 eV level would correspond to the thermal freeing of holes, that is, the thermal excitation of electrons from the valence band to the impurity level. If one takes the band gap value of GaAs at 300°K to be 1.43 eV (66W1, 69S2), then the level lies 0.79 eV below the bottom of the conduction band, in good agreement with the published values for the Cr level in GaAs (68A1, 68H1, 70K1, 71G1, 71K1, 72P1, 72P2, 73A1).

As explained by Schmidlin and Roberts (68S4), wide band-gap materials which have been compensated exhibit different activation energies

for the ohmic and non-ohmic region. The principal condition for this to apply however, is a field squared dependence of the current at high fields (or a space charge limited region). This is not the case here. However, the onset of F.D.T. may be inhibiting the space charge region formation at 300$^{o}$K since the field of 800 V/cm is fairly close to the threshold field (950 V/cm) for F.D.T. Below 300$^{o}$K, where no oscillations occur due to a decreasing $n\ell$ product, it may well be that the necessary field squared dependence does occur. This would then partly explain the superlinear behaviour of the current discussed in the last section. Since no measurements were taken of I-V between 90$^{o}$K and 300$^{o}$K, and since the high field value of 800 V/cm falls in a non-ohmic region near 300$^{o}$K, no definite interpretation of the 0.70 eV activation energy can be given here.

The 0.12 eV activation energy is also due to thermal freeing of holes. This places a partly filled acceptor level 0.12 eV above the valence band. This value is in fair agreement with published values (71C1) and is normally associated with copper as an acceptor in GaAs (61B1). As will be shown in the next section, the optical properties of the sample indicate the presence of a number of active levels which lie in close proximity to the valence band.

One further comment can be made concerning the data presented in Fig. 4-3. It can be seen that the break from the low temperature impurity level to the higher temperature impurity level occurs at approximately 225$^{o}$K. This value will reappear in the following sections when the optical properties and current oscillations are discussed.

## IV-2 Optical Properties

### 2.1 $I_p$-V Characteristics

At 300°K under the influence of 0.90μ radiation, the GaAs sample exhibited ohmic behaviour for applied fields up to $2 \times 10^3$ V/cm. No current oscillations were noted and no other anomalies were observed.

For an applied field of 100 V/cm, the value of current increased from $3 \times 10^{-8}$ A in the dark to about $2 \times 10^{-6}$ A under illumination, or almost two orders of magnitude. At 300°K, the 0.90μ radiation, with a resolution of ±0.01μ, would emit a sufficient amount of intrinsic radiation (0.89μ) to cause intrinsic carrier excitation and thus the increase in the current value.

Photo-Hall studies on the material by other workers (69M1, 72P4) indicate that the GaAs is strongly n-type at 300°K for illuminating radiation of wavelength 0.90μ to 1.15μ.

The situation is somewhat different at low temperatures (90°K). To begin with, the ratio of photocurrent to dark current for $\lambda = 0.90\mu$ becomes of the order of $10^7$, so that the effects of the dark current can be neglected. The ratio of $I_p$ to $I_d$ is not constant for all illuminating wavelengths however, as will be seen in the next section.

The $I_p$-V characteristics of the GaAs at 90°K, as illustrated in Fig. 4-4 fall into three distinct regions. Up to about 100 V/cm, the material has an ohmic behaviour. This begins to deviate above 100 V/cm and as was the case at 300°K in the dark, the current begins to exhibit sublinear behaviour. The current reaches a saturation value of 250 V/cm, and from there up to 750 V/cm it decreases gradually, clearly illustrating

Fig. 4-4 Photocurrent-Electric Field Characteristics at 90$^{\circ}$K

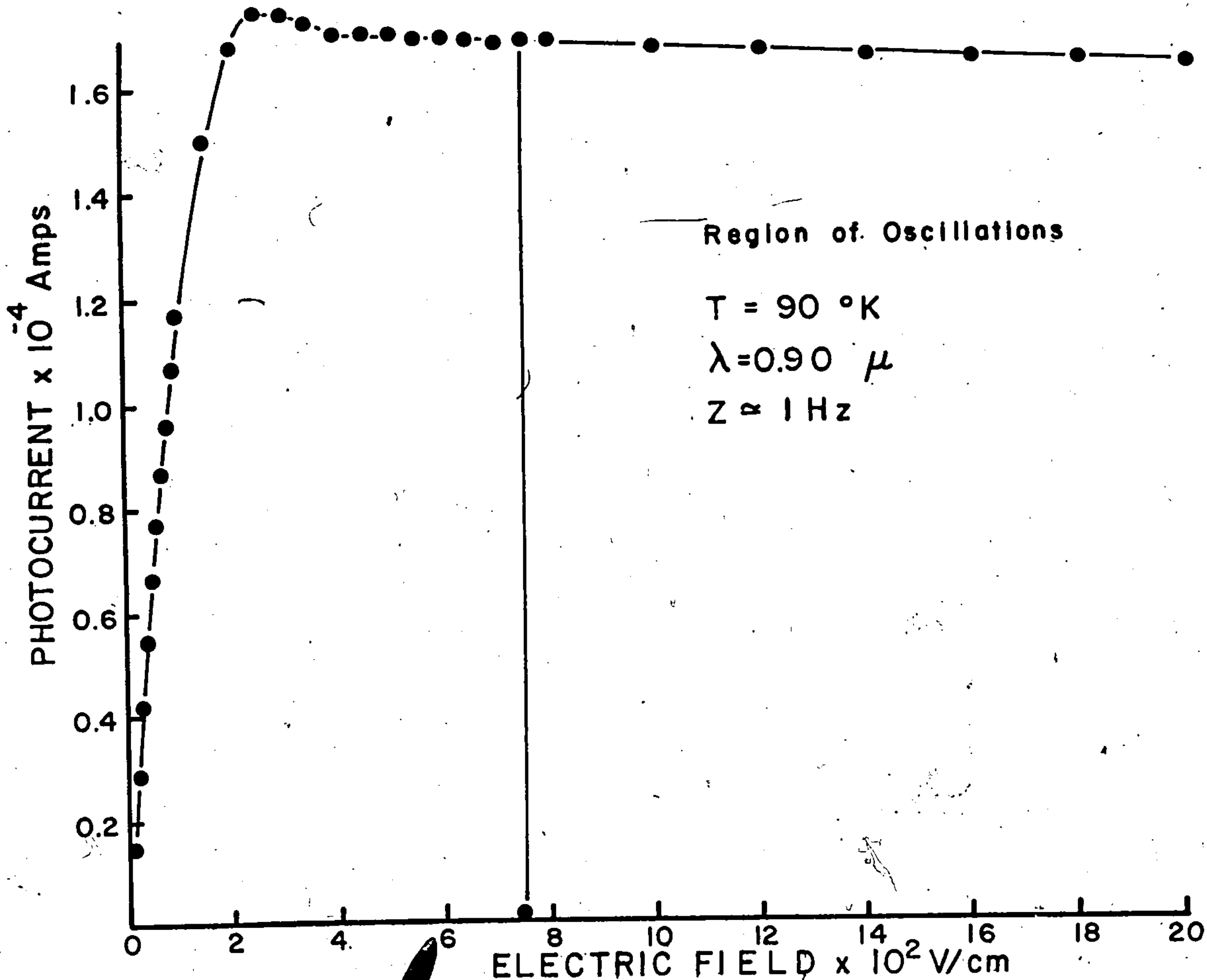
Region of Oscillations
T = 90 °K
λ=0.90 μ
Z ≈ 1 Hz
PHOTOCURRENT x 10-4 Amps
1.6
1.4
1.2
1.0
0.8
0.6
0.4
0.2
0
2
4
6
8
10
12
14
16
18
20
ELECTRIC FIELD x 10² V/cm

the region of N.D.R. The non-linear saturating and then decreasing behaviour is due to the increasing effectiveness of the F.D.T. mechanism at higher fields.

Above the threshold field (750 V/cm) the current oscillates (frequency $\sim$ 1 Hz) as domains form and then travel across the sample, as explained in Chapter II. Note that the peak value of current continues to (very) gradually fall as the field is increased up to $2 \times 10^3$ V/cm.

Since the number of carriers is much larger at $90^{\circ}$K under light excitation than at $300^{\circ}$K in the dark (the $I_p$ to $I_d$ ratio was about $10^2$ at $300^{\circ}$K), the field in the domains (and hence the difference between the high and low values of current) is now much larger. Subsequently, all low current values read essentially zero for the scale used in Fig. 4.4

Note that the operating field used in this work to study the oscillations (800 V/cm) is just above the threshold value needed to generate the oscillations. A higher value, however, would have been in the non-ohmic region of the dark current, so the 800 V/cm value was felt to be an adequate compromise between the two limiting factors.

The role of the 0.90μ radiation and how it induces a high free carrier concentration will be discussed in a subsequent section.

Since photo-conduction at $90^{\circ}$K is strongly n-type, it is possible to calculate from the data in Fig. 4-4 the minimum $n\ell$ product needed for the onset of current oscillations. Using $\mu_n = -2.0 \times 10^4 cm^2/V$ sec (72P4), for a current of $1.7 \times 10^{-4}$ A and a threshold field of $7.5 \times 10^2$ V/cm, one obtains a value for $n\ell$ of $3 \times 10^9$ $cm^{-2}$. This value is larger than the one calculated at $300^{\circ}$K ($n\ell \sim 10^7 - 10^8$ $cm^{-2}$).

As will be shown in a later section, when intensity (rather than field) is used to control the onset of oscillations, the minimum $n\ell$ product obtained is consistent with the above value.

2.2 Spectral Response

Fig. 4-5 illustrates the spectral response of the sample at 300°K for wavelengths near the gap value under both low and high field conditions. Except for the peak due to intrinsic excitation, there is only one other structure present. This is a broad peak with band edge trailing in the 0.96μ to 1.00μ range. It is not too apparent at low fields but becomes slightly more pronounced at higher fields.

There is some difficulty in deriving an activation energy from this data due to the width of the level. Since the impurity response comprises a broad maximum followed by an exponential tail, it would seem valid to take as an "optical activation energy" for the level the energy corresponding to the wavelength at the half maximum of the sensitivity response (52M1). This yields an activation energy of 1.01 eV.

The photo-Hall mobility in this region is negative (-4[illegible]200 $cm^2$ $(V\ sec)^{-1}$ (72P4)) which indicates the conductivity is due mainly to electrons. This suggests the existence of a fairly high density of levels, containing electrons, situated 1.01 eV above the conduction band, or 0.42 eV above the valence band. These deep levels are most probably compensated acceptors and may be the ones responsible for the high resistance of the sample (and for the current oscillations, as will be discussed in a later section).

Fig. 4-5 Spectral Response at 300$^{o}$K for High and Low Field Conditions

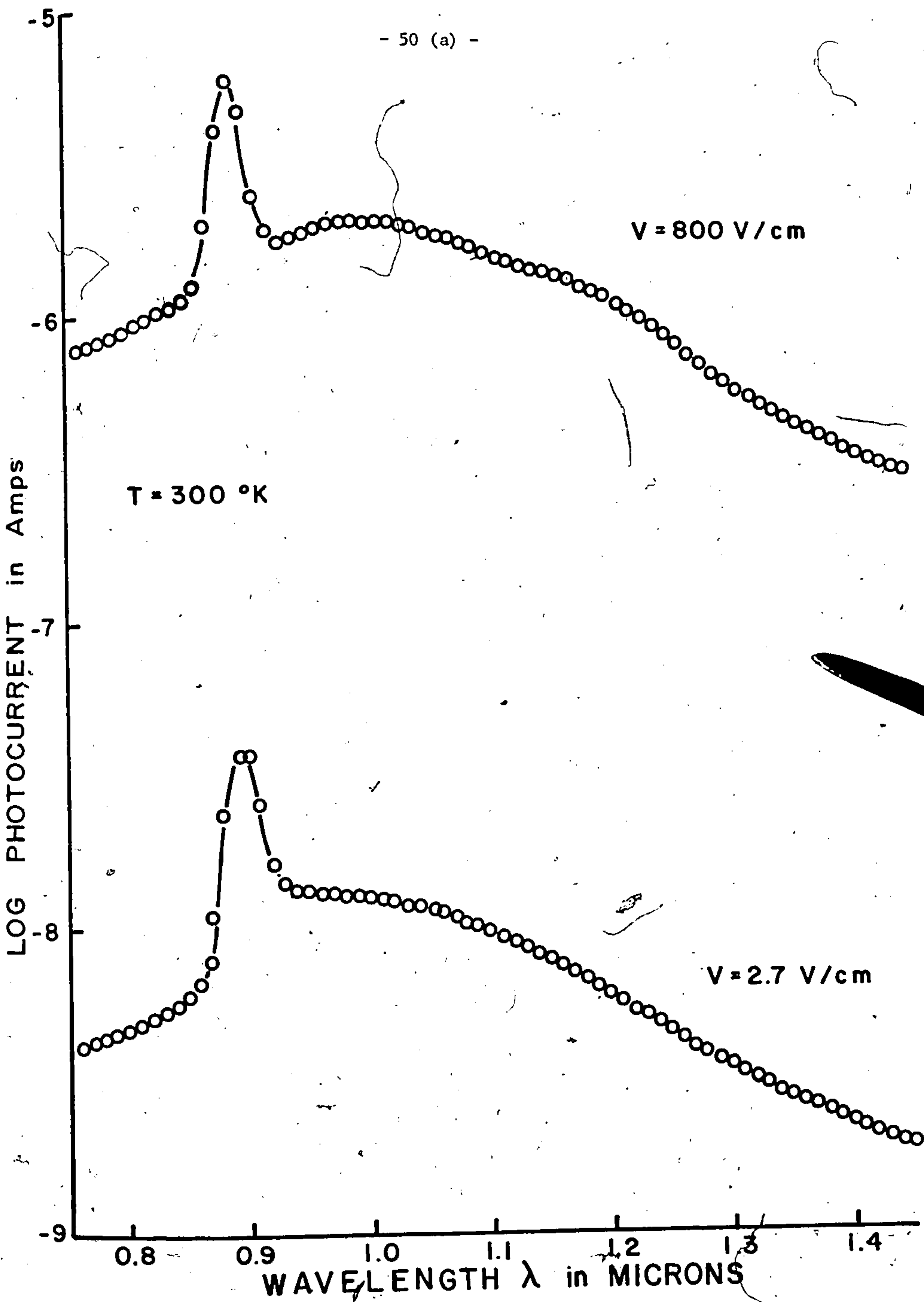

V = 800 V/cm
T = 300 °K
V = 2.7 V/cm
LOG PHOTOCURRENT in Amps
-5
-6
-7
-8
-9
0.8
0.9
1.0
1.1
1.2
1.3
1.4
WAVELENGTH λ in MICRONS

At 90$^{\circ}$K, under low field conditions, the spectral response of the GaAs crystal shows several regions of interest, as illustrated in Fig. 4-6.

The first and highest peak corresponds to the intrinsic transitions, yielding the band gap value of 1.51 eV. The decrease in the sensitivity at higher energies ( $\lambda < 0.82\mu$) may be attributed to an increase in the absorption coefficient resulting in an increase in the fraction of carriers recombining at the surface of the material (69M1).

At photon energies less than the band gap, the response falls due to fact that the creation of electron-hole pairs ceases. There is a peak at 0.90μ (1.36 eV) which is due to the photo-excitation of electrons from an impurity level to the conduction band, since it is known that the current in this region of wavelength is n-type, even though mixed conduction is present (72P4). This would place the impurity level 0.15 eV above the valence band, in good agreement with published results (64B1, 66S1, 66S2, 72B2), and is due to copper impurities in the sample which are inadvertently introduced during preparation.

It will be shown in a later section that this copper impurity plays a role in the current oscillations.

The peak at 1.28μ corresponds to an activation energy of 0.97 eV. Again due to the electronic nature of the conduction process at this wavelength, the peak is associated with a partly filled level 0.54 eV above the valence band. Such a level is usually attributed to either copper impurities or a lattice defect, and has been observed both in Cr-doped GaAs (69V1) and in GaAs compensated by other means (66F1, 67S1).

No real meaning will be assigned as yet to the valley at 1.16μ, corresponding to an activation energy of 1.06 eV, but its significance will be made clear when the discussion of the quenching of current oscillations is given.

Note that the scanning in Fig. 4-6 begins from the low energy end and goes up in energy. As well, the scanning had to be done by fixed increments of wavelength, each reading taking up to one hour to stabilize. A fast scan from the high energy end yields only a broad peak between 0.84μ and 1.00μ, as illustrated in Fig. 4-7. This suggests that some type of slow process is involved, and its interpretation is the subject of another work (72P4).

Spectral scans at high fields were attempted. However, the appearance of oscillations at certain wavelengths prevented any meaningful data from being obtained.

### 2.3 Variation of Photocurrent with Temperature for Selected Wavelengths

Because of interest in the roles the various impurity levels might play in the current oscillations, the behaviour of the photocurrent with temperature was measured for the wavelengths corresponding to the extrinsic peaks mentioned in the last section (0.90μ and 1.30μ). As well, the effect that radiation of 1.16μ wavelength might have on the photocurrent was also measured since this radiation was found to be responsible for the quenching of the oscillations. The results are illustrated in Fig. 4-8. The 0.90μ radiation will be considered first.

Fig. 4-6 Spectral Response at $90^{o}K$ under Low Field Conditions-Scan Up

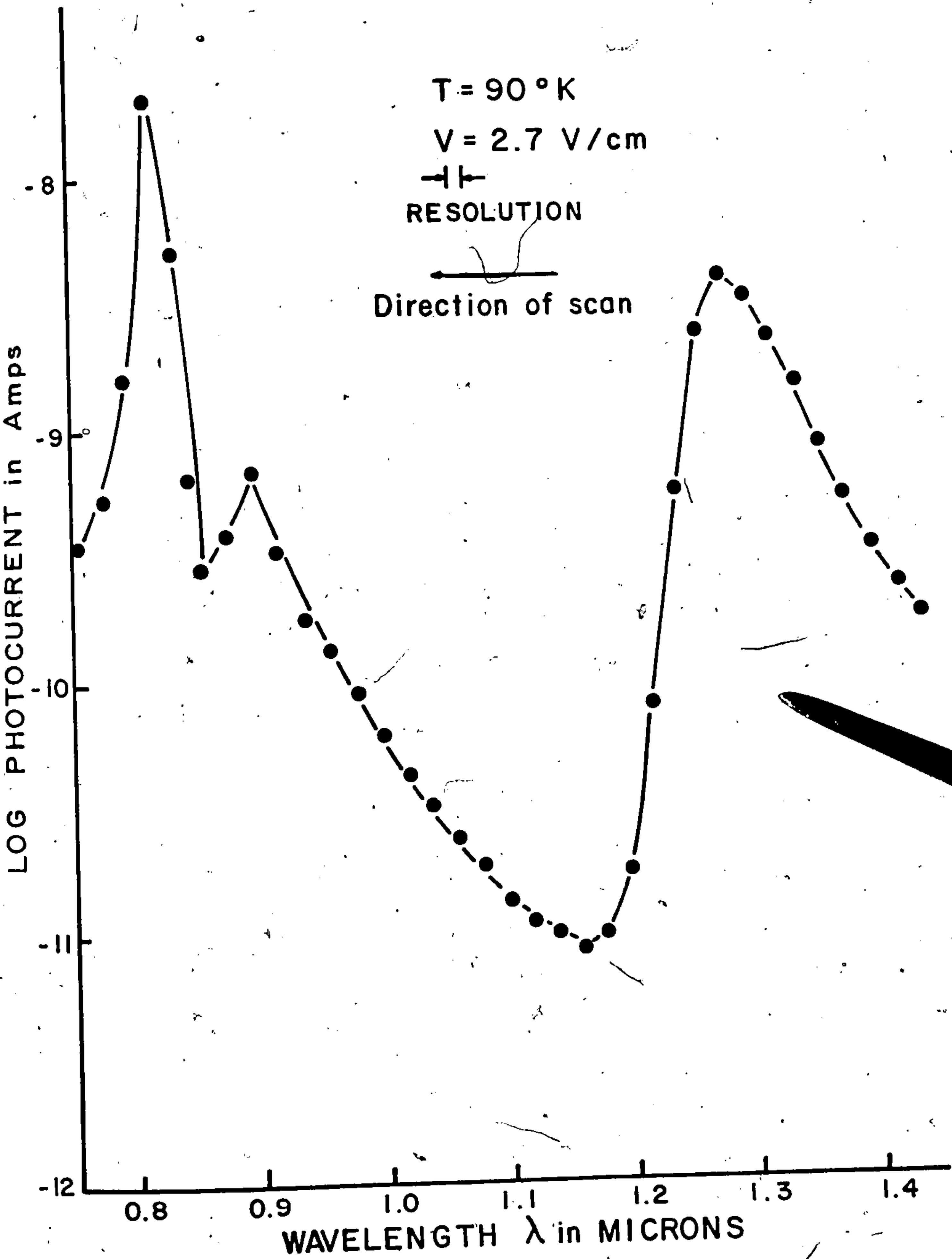
T = 90 °K
V = 2.7 V/cm
RESOLUTION
Direction of scan
LOG PHOTOCURRENT in Amps
-8
-9
-10
-11
-12
0.8
0.9
1.0
1.1
1.2
1.3
1.4
WAVELENGTH λ in MICRONS

Fig. 4-7 Spectral Response at $90^{o}K$ under Low Field Conditions-Scan Down

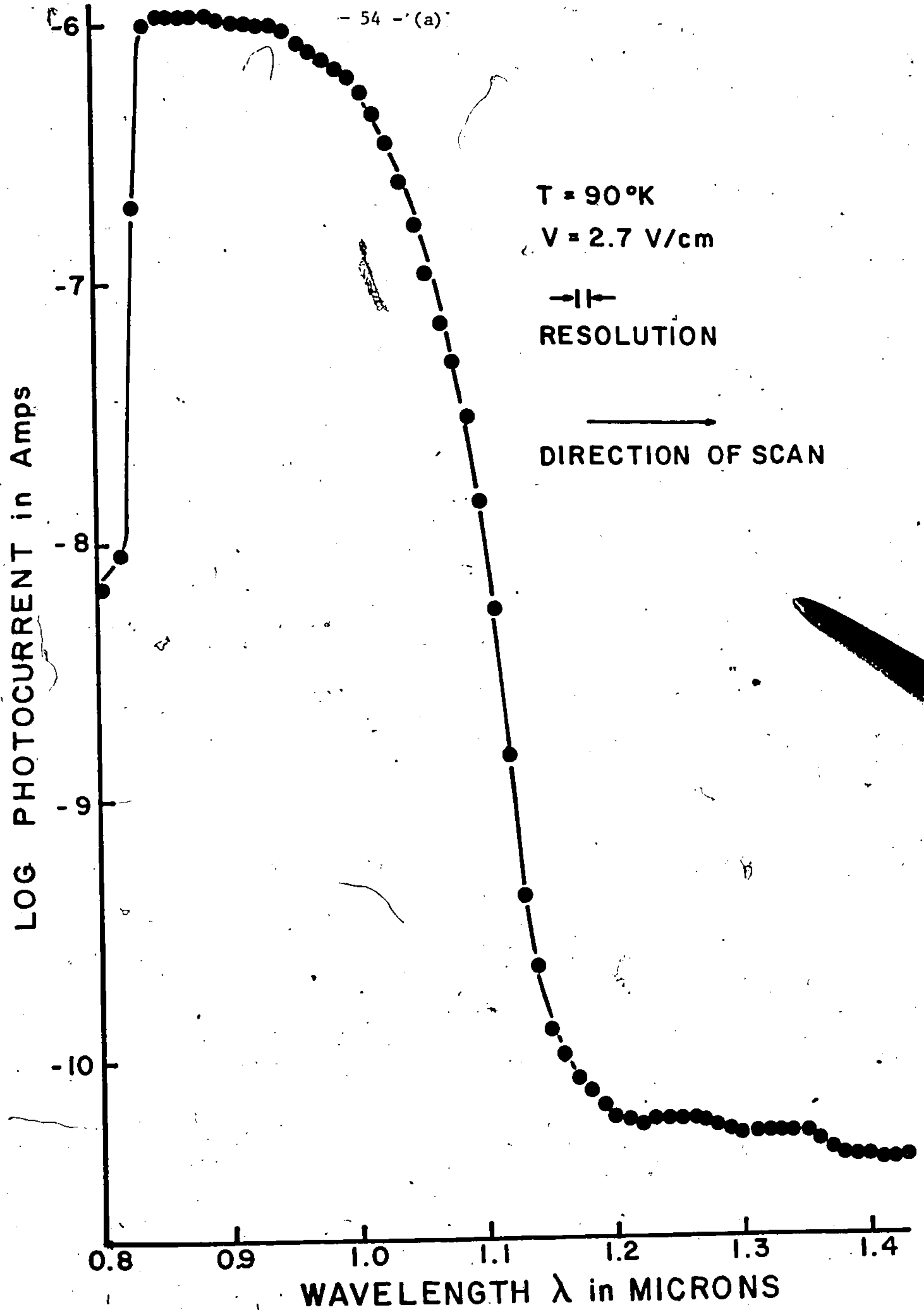
-6
-7
-8
-9
-10
LOG PHOTOCURRENT in Amps
T = 90°K
V = 2.7 V/cm
RESOLUTION
DIRECTION OF SCAN
0.8
0.9
1.0
1.1
1.2
1.3
1.4
WAVELENGTH λ in MICRONS

Fig. 4-8 Photocurrent as a Function of Temperature Under Low Bias Condition for Various Wavelengths

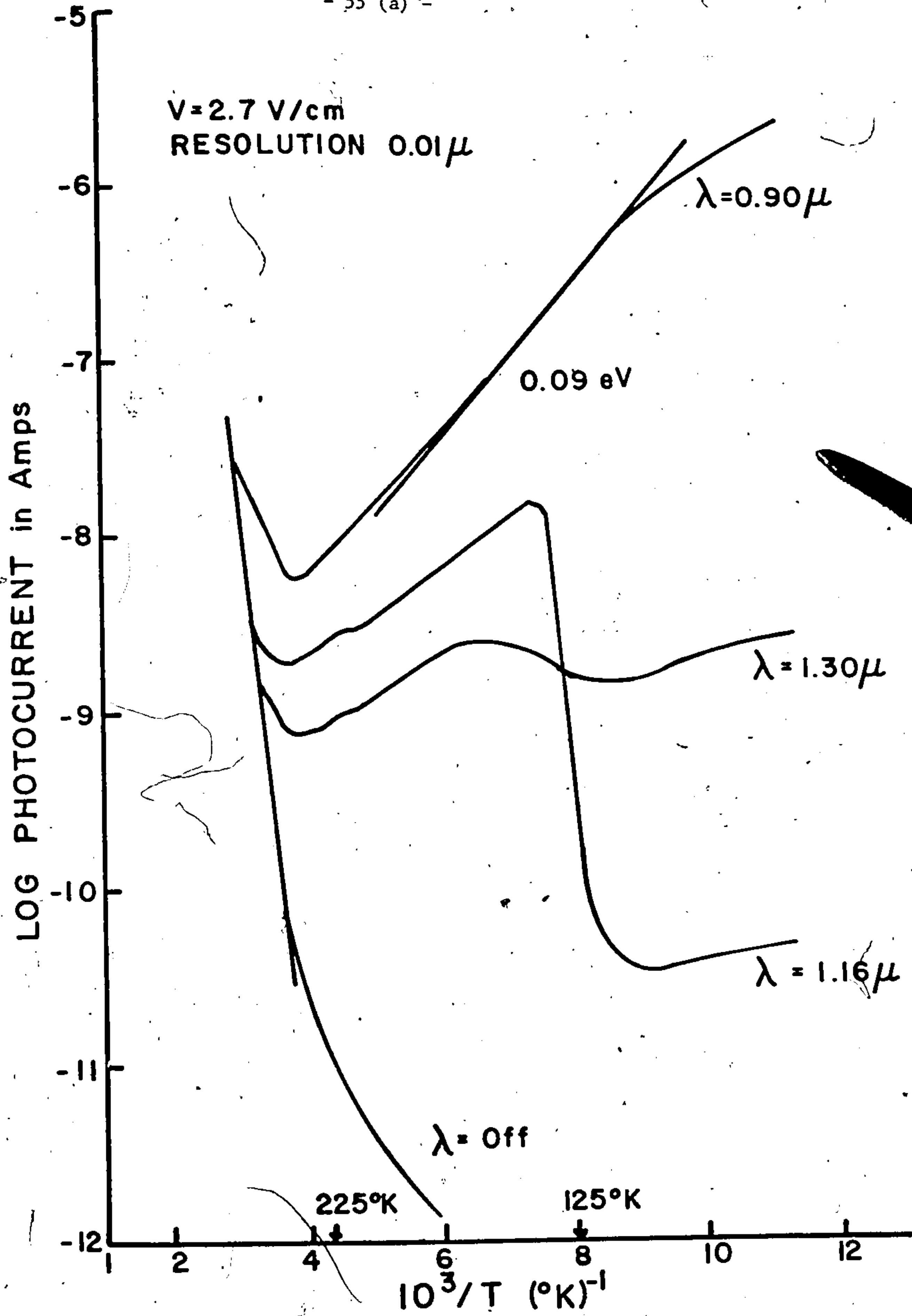
V=2.7 V/cm
RESOLUTION 0.01μ
λ=0.90μ
0.09 eV
λ=1.30μ
λ=1.16μ
λ= Off
225°K
125°K
LOG PHOTOCURRENT in Amps
-5
-6
-7
-8
-9
-10
-11
-12
1
2
4
6
8
10
12
10³/T (°K)⁻¹

2.3.1 0.90μ

It can be seen from Fig. 4-8 that when the GaAs is illuminated with 0.90μ radiation, it becomes sensitized since the photocurrent at 90°K is 2 x $10^2$ times larger than at 300°K. This increase in photocurrent at low temperatures can be explained with the aid of the theory of sensitizing centres presented in Chapter II.

For GaAs at 90°K, 0.90μ radiation lies in the extrinsic range. Thus the 0.15 eV impurity level must be contributing the carriers. Other workers have shown that the material is n-type at 90°K under 0.90μ illumination, and that the conduction is mixed with n ∿ p. To explain this one needs to postulate a model based on double excitation. Such a model is shown in Fig. 4-9.

Level II would be the level just mentioned, while level I would have to be an empty (due to compensation) donor level located about 0.15 eV below the conduction band. Such a donor level has been reported for GaAs (66B1, 66S2). Centres s and r are the fast and slow recombination centres of the type described in Chapter II. Initially (dark at 90°K) level I and centres s are empty, while level II and centres r are partially filled. Upon illumination with 0.90μ radiation, double excitation occurs, as illustrated by transitions (1) and (2). The hole created by transition (2) is captured by centre r (transition (5)). The electron, which is now in level I has two possibilities; it may be trapped by the fast centres s (transition (3)), or it may be trapped at level II (transition (4)). It is not likely to be trapped by the r centres because of the nature of that centre, that is, because the r centres have a small capture cross-

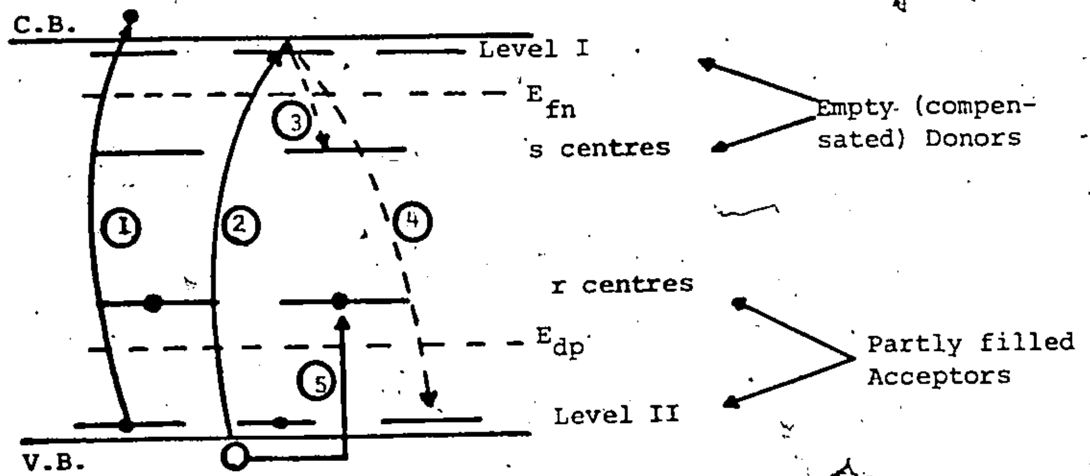


Fig. 4-9 Model for Double Exciation and Sensitizing Mechanism in GaAs.

section for free electrons.

If transition (4) occurs (level I to level II), the electron will be excited into the conduction band by the 0.90μ radiation and will thus contribute to the photocurrent. Transition (3) (level I to the s centres) will result in the s centres becoming occupied principally by electrons. Thus most of the electrons initially in the r centres are effectively transferred to the s centres.

The net effect is thus the same as described in Chapter II. Once the system has reached steady state, the lifetime of the free electron is increased since it now faces mainly centres with a small capture cross section (r centres) and only a few centres with large capture cross section (s centres). The net effect is a large increase in the mixed conduction and hence the photoconductivity of the material. As will be seen, this model also explains in part the characteristics of the curve due to the 1.16μ radiation in Fig. 4-8.

2.3.2 1.16μ

Again from Fig. 4-8, it can be seen that the 1.16μ radiation quenches the photocurrent at temperatures below ∿ 125°K. The reason for this can be explained in terms of the model just discussed.

At temperatures higher than ∿ 125°K, the hole demarcation level lies above the level containing the r centres (Chapter II, section 3). The 1.16μ radiation would excite electrons to the conduction band and the level with the r centres would behave as an ordinary impurity level resulting in impurity photoconductivity.

As the temperature is decreased however, the hole demarcation level level shifts towards the valence band. At a certain temperature (∿ 125°K in this case) it crosses the impurity level. This changes the nature of the r centres in the level. They now effectively present a small capture cross section for electrons, so that electrons being excited to the conduction band are not likely to recombine at the r centres. Instead they are trapped at the s centres which have large capture cross sections for free electrons.

Effectively, most of the electrons formerly in the r centres are transferred to the s centres. Since there are no other free carriers being generated, the photocurrent decreases rapidly.

Since thermal quenching occurs when the hole demarcation level crosses the acceptor level containing the r centres, the depth of the acceptor level $E_r$ as measured from the valence band can be written as

$$E_r = kT \ln \left(\frac{s_p}{s_n} \frac{N_v}{n}\right) \qquad (60B1)$$

where $s_n$ = capture cross section for electrons

$s_p$ = capture cross section for holes

$N_v$ = density of states in the valence band

$n$ = electron concentration.

Assuming the ratio of $s_p/s_n$ to be about $10^7$ (67S1) kT ∿ 0.01 eV (for 125°K) and n ∿ $10^9/cm^{-3}$ the value of $E_r$ is estimated to be ∿ 0.4 eV. Such a level has been reported and is attributed to a lattice defect (72B1).

The 1.16μ radiation quenches the current oscillations at 90°K. This quenching effect holds true only for temperatures below ∿ 125°K. As will be shown, this behaviour is consistent with the model described above.

2.3.3 1.30μ

Under the influence of 1.30μ radiation, the photocurrent shows only slight variation with temperature up to ∿ 250°K. It then increases exponentially as the dark current becomes predominant. The photocurrent is due to electron excitation (material is n-type) to the conduction band from the level (0.54 eV above the valence band) identified optically in a previous section.

In the range ∿ 125°K to ∿ 225°K, all three photocurrents decrease in value as the temperature rises. Above ∿ 225°K, the three photocurrents increase as the dark current begins to be dominant. No detailed investigation of this range of temperature was performed in this work.

For the 0.90μ radiation, the decrease in photocurrent in the ∿ 125°K to ∿ 225°K temperature range is exponential. The activation energy associated with this decrease, 0.09 eV, has been reported for high resistivity GaAs by a number of workers as being due to copper acceptor impurities located just above the valence band (62Bl, 72Pl).

2.4 Energy Levels

The energy values for the impurity levels at 300°K and 90°K determined in this research are shown in Fig. 4-10.

All energies are measured from the top of the valence band. The levels marked I, II, s and r are believed to correspond to the ones discussed in the double excitation carrier generation model.

The impurity level corresponding to the r centres has been assigned the value of 0.45 eV on the basis of the valley found in the spectral response and the fact that the 1.16μ radiation quenches the oscillations and the photocurrent.

If one assumes that the impurity levels shift slightly ( ∿ 10%) as the temperature decreases, the shift being away from the band edges, then the 0.12 eV level at 300°K may correspond to the 0.15 eV level at 90°K. However, this requires a 20% shift in energy which seems rather high. A 7% shift in energy would place the 0.42 eV level (at 300°K) at 0.45 eV when the sample was cooled to 90°K, so that these two levels are believed to be the same one.

IV-3 Current Oscillations and Quenching

3.1 Dependence of the Current Oscillations on

3.1.1 Temperature

A. Photocurrent: Fig. 4-11 illustrates the temperature dependence of the photocurrent for high field conditions. The two curves correspond to the maximum ($I_p$max) and minimum ($I_p$min) values of photocurrent during the oscillations. At low temperatures (∿ 90°K) the two

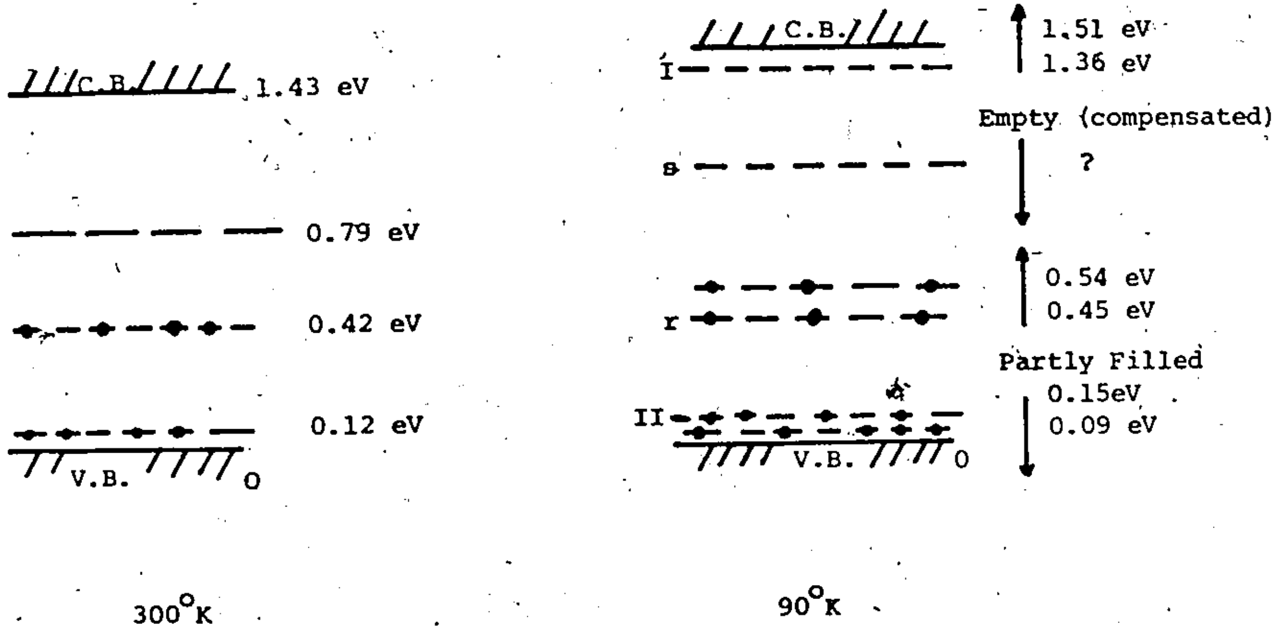


Fig 4-10 Energy Distribution for Impurity Levels in Semi-insulating GaAs at 300°K and 90°K

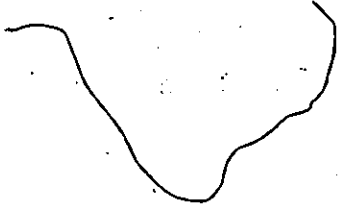

Fig. 4-11 Photocurrent as a Function of Temperature Under High Field Conditions.

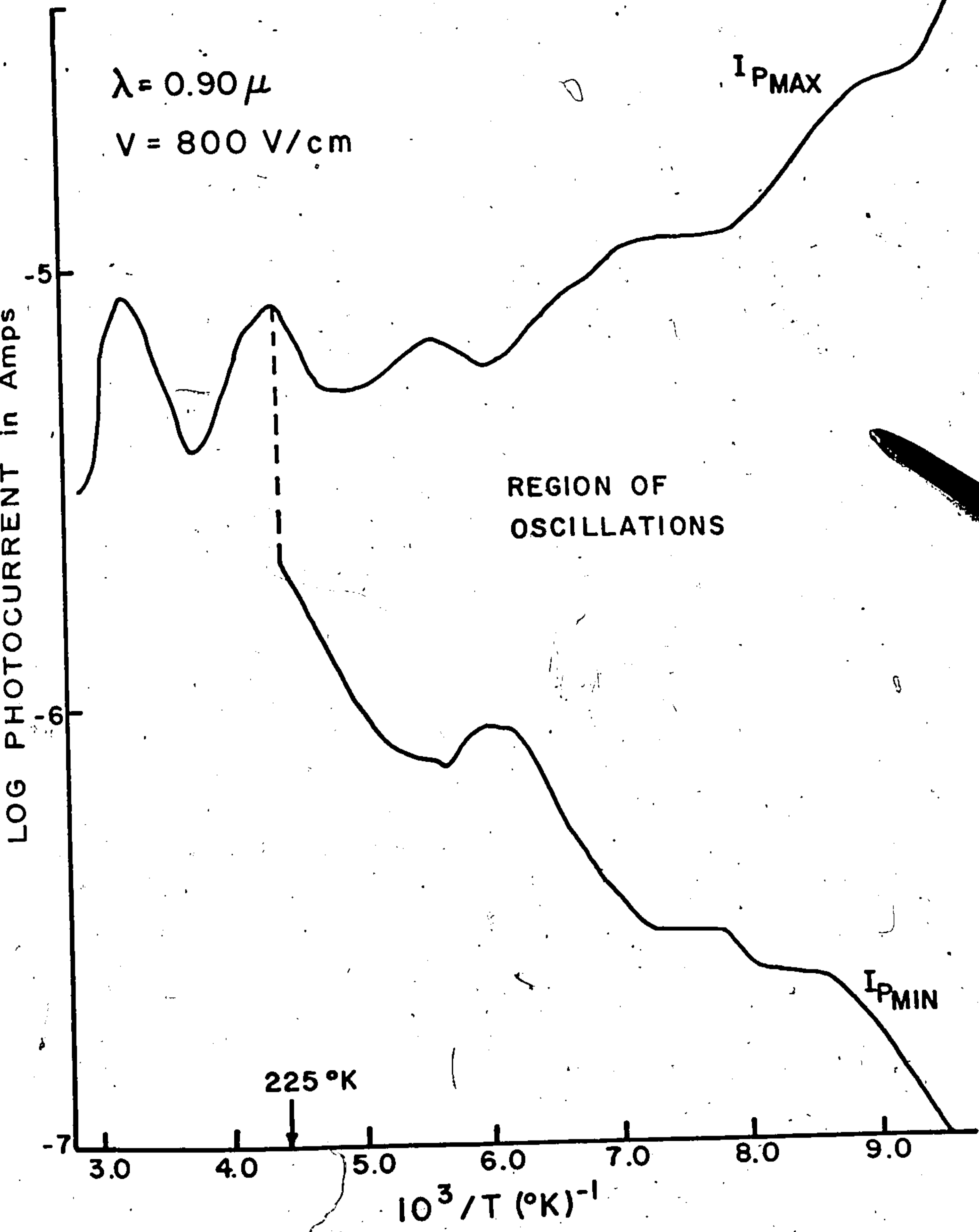

λ = 0.90 μ
V = 800 V/cm
$I_{P_{MAX}}$
REGION OF OSCILLATIONS
$I_{P_{MIN}}$
LOG PHOTOCURRENT in Amps
-5
-6
-7
225 °K
3.0
4.0
5.0
6.0
7.0
8.0
9.0
$10^3/T\ (°K)^{-1}$

values differ by a ratio of about $10^4$ but this ratio decreases as the temperature is increased. This behaviour is believed to be due to the fact that as the temperature rises, the $n\ell$ product required for domain formation decreases. The result would be smaller values of field in the domain (and larger ones in the region outside the domain).

That the minimum $n\ell$ product required for domain formation decreases as one increases the temperature of the sample can be seen if one considers the temperature at which the oscillations stop, in this case $225^{o}K$. (This value of temperature has been mentioned in previous sections when discussing electrical and optical properties of the material). Using $I_{p}max = 8.0 \times 10^{-6}A$ at $225^{o}K$, for a field of $8.0 \times 10^{2}$ V/cm, and $\mu_n \sim -1.0 \times 10^{4}\ cm^{2}(V\ sec)^{-1}$, one obtains a value for $n\ell$ of $3 \times 10^{8}\ cm^{-2}$.

Table 4-1 summarizes the behaviour of the minimum $n\ell$ product as a function of temperature.

One possible explanation for the behaviour illustrated in Table 4-1 is that the F.D.T. becomes more effective as the temperature of the sample is increased. If this were the case, then one would expect that the period of the oscillations would decrease (or the frequency increase) as the effectiveness of the trapping increased. This would be due to the fact that the domains could traverse the length of the sample in a shorter period of time. This assumes that the domain size is much smaller than the sample length and does not change appreciably as the temperature is increased. As well, it assumes a growth time for the domains much smaller than the period of the oscillations. Growth times of domains in GaAs have been reported in the range of $10^{-6}$ sec (72T1), which is considerably shorter

Table 4-1 Variation of Minimum $n\ell$ Product with Temperature

| Temperature $^{o}K$ | Radiation $\mu$ | $n\ell$ Product $cm^{-2}$ | Controlling Parameter |
|---|---|---|---|
| 90 | 0.90 | $\sim 2 \times 10^{9}$ | Radiation Intensity |
| 90 | 0.90 | $\sim 3 \times 10^{9}$ | Electric Field |
| 225 | 0.90 | $\sim 3 \times 10^{8}$ | Temperature |
| 300 | Dark | $\sim 5 \times 10^{7}$ | Electric Field |

than the period of the oscillations obtained in this work (1 sec. to $10^{-2}$ sec).

B. Period: The behaviour of the period as a function of temperature is illustrated in Fig. 4-12. The graph shows that the period of oscillations is fairly constant at $\sim$ 1 sec for temperatures below $\sim 125^{o}K$. It begins to decrease between $\sim 125^{o}K$ and $\sim 160^{o}K$, and then decreases exponentially from a value of $\sim 8 \times 10^{-1}$ sec to $\sim 6 \times 10^{-3}$ sec, or until the oscillations stop at $225^{o}K$. If the exponential fall at higher temperatures is associated with an activation energy, the value of this energy is found to be 0.21 eV. While this behaviour for the frequency of the current oscillations in GaAs has been reported (but with different activation energies) (69S1), the following interpretation has not been presented before.

For fixed intensity of illumination and applied field the motion of the domains across the length of the sample will be determined principally by two factors: the number of free carriers n (electrons) available for the F.D.T. process, and the probability P of these carriers being captured at an impurity centre through the F.D.T. mechanism. The product of these two factors, nP, will determine the velocity of the domains, and thus the period t of the oscillations.

The number of free carriers available in this case is determined by the temperature dependence of the photocurrent due to the 0.90μ radiation. Thus

$$n \propto e^{+\frac{E_n}{kT}}$$

where $E_n$ = 0.09 eV as determined from Fig. 4-8 in section 2.3 of this Chapter.

Fig. 4-12 Temperature Dependence of the Period of Oscillation

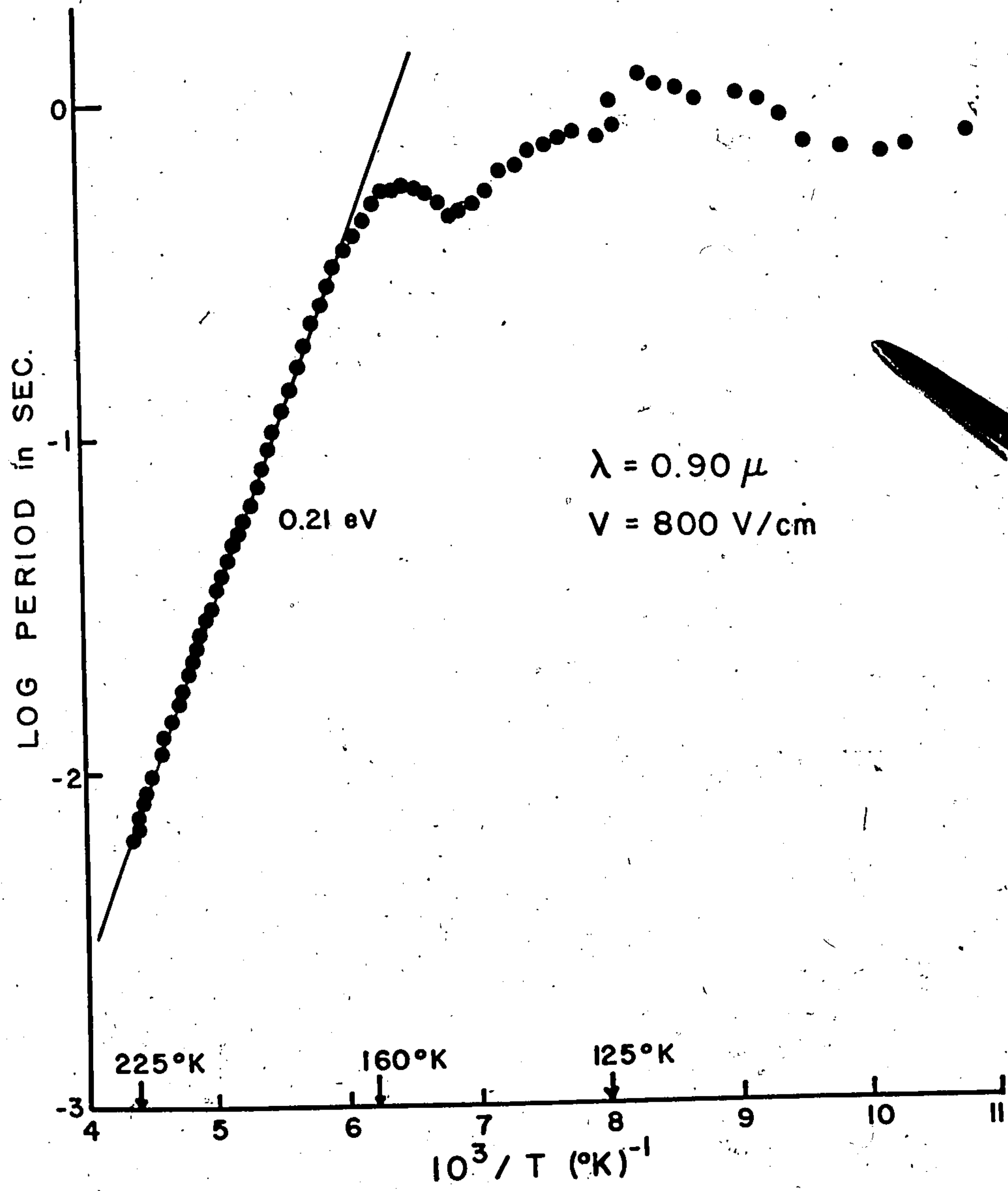

LOG PERIOD in SEC.
0
-1
-2
-3
0.21 eV
λ = 0.90 μ
V = 800 V/cm
225°K
160°K
125°K
4
5
6
7
8
9
10
11
10³/ T (°K)⁻¹

The probability of a carrier being captured through F.D.T. will depend on the barrier height $\phi$ presented to the electron by the impurity centre. The temperature variation of the capture probability will be (see Appendix)

$$P \propto e^{-\frac{\phi}{kT}}$$

Thus the velocity v of the domain will be given by

$$v \propto nP \propto e^{-\frac{-E_n + \phi}{kT}} \qquad \text{I}$$

The period of the oscillations t decreases as the temperature increases, so that

$$t \propto e^{+\frac{E_A}{kT}} \qquad \text{II}$$

where $E_A$ is the activation energy found in Fig. 4-12 and has the value of 0.21 eV.

Since the period is inversely proportional to the velocity, then (I) and (II) yield

$$-E_A = -(-E_n + \phi)$$

Substituting the values of $E_A$ and $E_n$ gives

$$\phi = 0.30 \text{ eV}$$

This value of $\phi$ satisfies the condition that the barrier height be $> 0.08$ eV.

Barrier heights of 0.2 eV in n-type Ge containing $Au^{--}$ centres have been reported by Ridley and Pratt (65R2), while in the investigation of GaAs:Au Schottky barriers, potential barriers of 0.2 eV at deep centres have been reported by Senechal and Basinski (68S2). Thus the value of 0.30 eV found in this work for a barrier height seems reasonable. However, further experimental evidence would be required before one could positively attribute this energy to the repulsive Coulomb barrier responsible for F.D.T.

3.1.2 Intensity of Illumination

The behaviour of the frequency of oscillations with changing intensity of the 0.90μ radiation is illustrated in Fig. 4-13.

This behaviour is consistent with the explanation given in Section 3.1.1B for the temperature dependence of the period of oscillations. Since the period of oscillation at fixed temperature (90°K), field (800 V/cm) and illuminating radiation (0.90μ) would depend solely on the carrier concentration, an increase in carrier concentration results in a decrease in the period. Thus the period will be inversely proportional to the intensity, or a linear relationship exists between the frequency, and the intensity, as found in Fig. 4-13.

The maximum carrier concentration available for domain formation and progress would also be determined by the intensity. Thus the maximum current during oscillations will be linear with intensity. This is illustrated in Fig. 4-14.

Since the intensity controls the free carrier concentration, it

Fig. 4-13. Frequency of Oscillation as a Function of Intensity at 90°K

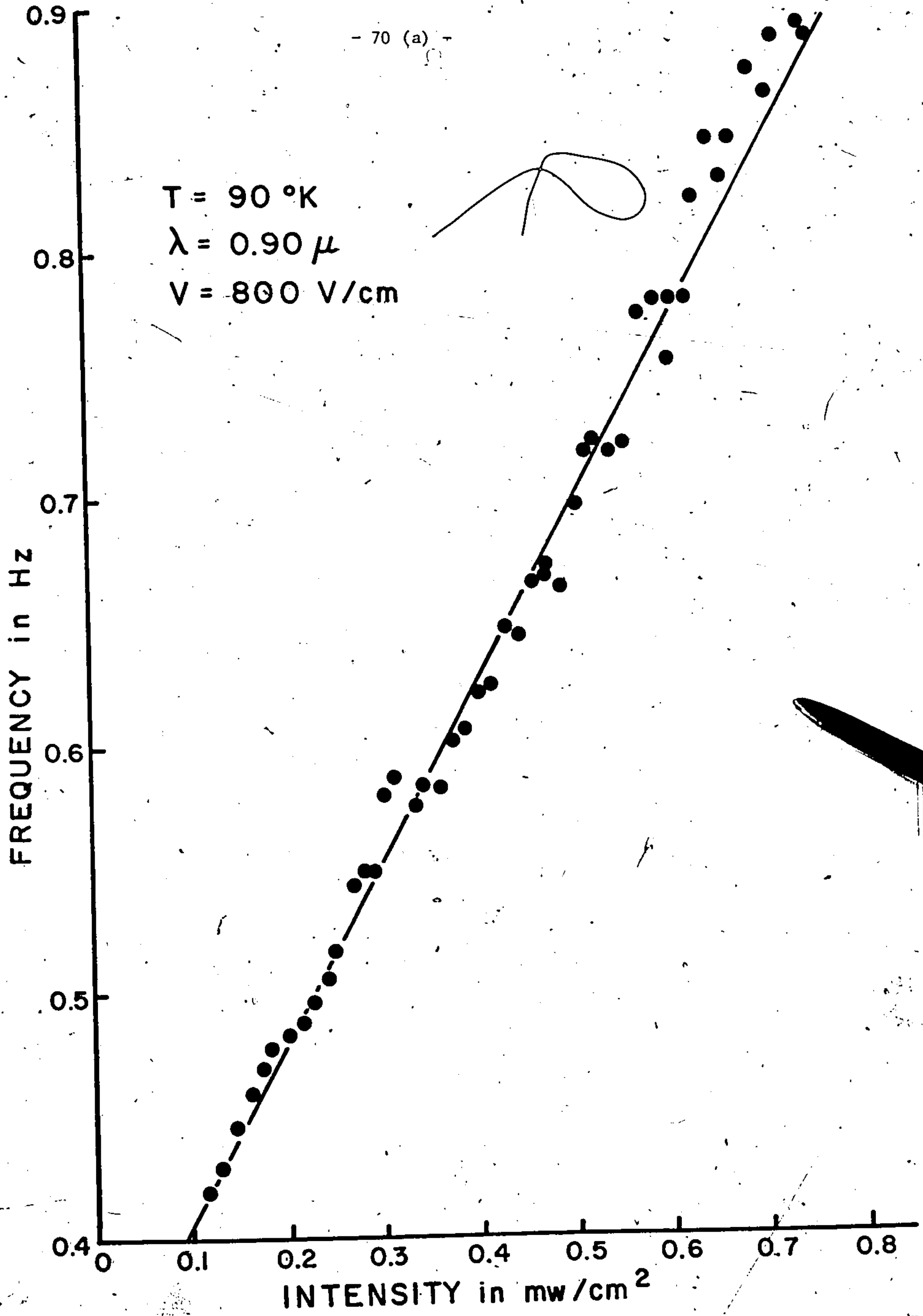
T = 90 °K
λ = 0.90 μ
V = 800 V/cm
FREQUENCY in Hz
0.9
0.8
0.7
0.6
0.5
0.4
0
0.1
0.2
0.3
0.4
0.5
0.6
0.7
0.8
INTENSITY in mw/cm2

Fig. 4-14 Maximum Photocurrent as a Function of Intensity at $90^{o}K$

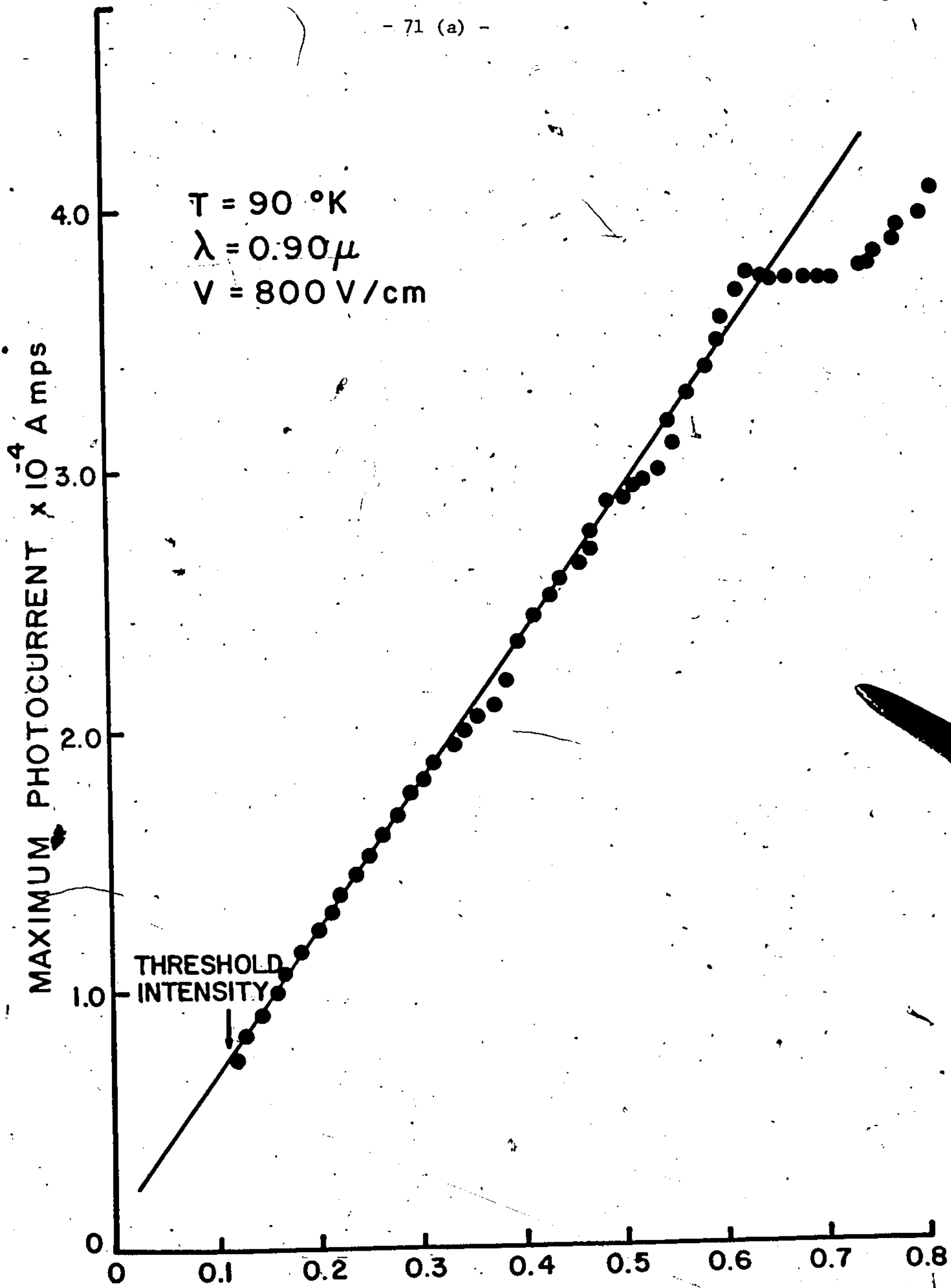
T = 90 °K
λ = 0.90μ
V = 800 V/cm
MAXIMUM PHOTOCURRENT x 10⁻⁴ Amps
THRESHOLD INTENSITY
0
1.0
2.0
3.0
4.0
0
0.1
0.2
0.3
0.4
0.5
0.6
0.7
0.8
INTENSITY in mw/cm²

will also control the minimum $n\ell$ value required for domain formation. From Fig. 4-14 one can obtain the minimum value of current needed to generate the oscillations, $7.3 \times 10^{-5}$A. Using $\mu_n = -2.0 \times 10^{4}$ $cm^{-2}$ $(V\ sec)^{-1}$ and $E = 8.0 \times 10^{2}$ V/sec, one obtains a value for $n\ell$ of $2 \times 10^{9}$ $cm^{-2}$. This is in good agreement with the value of $3 \times 10^{9}$ $cm^{-2}$ obtained for the threshold voltage in section 2.1.

### 3.1.3 Wavelength of Illumination

A manual scan from the high energy end of the spectrum (0.70μ) determined a region of existence for the oscillations between 0.85μ and 0.96μ as illustrated in Fig. 4-15. Above 0.96μ it was found that the oscillations were quenched and that the photocurrent decreased by about three orders of magnitude. The rise in the photocurrent (and the onset of oscillations) near the band gap is attributed to the generation of charge carriers by excitation across the gap, or by excitation from the 0.15 eV level near the valence band. At lower energies the radiation either fails to create the necessary number of free carriers required for domain formation ($n\ell$ product), or it empties the 0.45 eV sensitizing centres (for wavelengths near 1.16μ) thereby quenching both the oscillations and the photocurrent (as will be explained in a later section).

Note the similarity in the shape of this curve and the one obtained at low fields, when scanning also started from the high energy end (Fig. 4-7). The main difference is the presence of a broader peak (extending to about 1.05μ) in the low field scan. The reason for the appearance of such broad peaks (in both low and high fields cases) is

Fig. 4-15 Spectral Response at 90°K under High Field Conditions

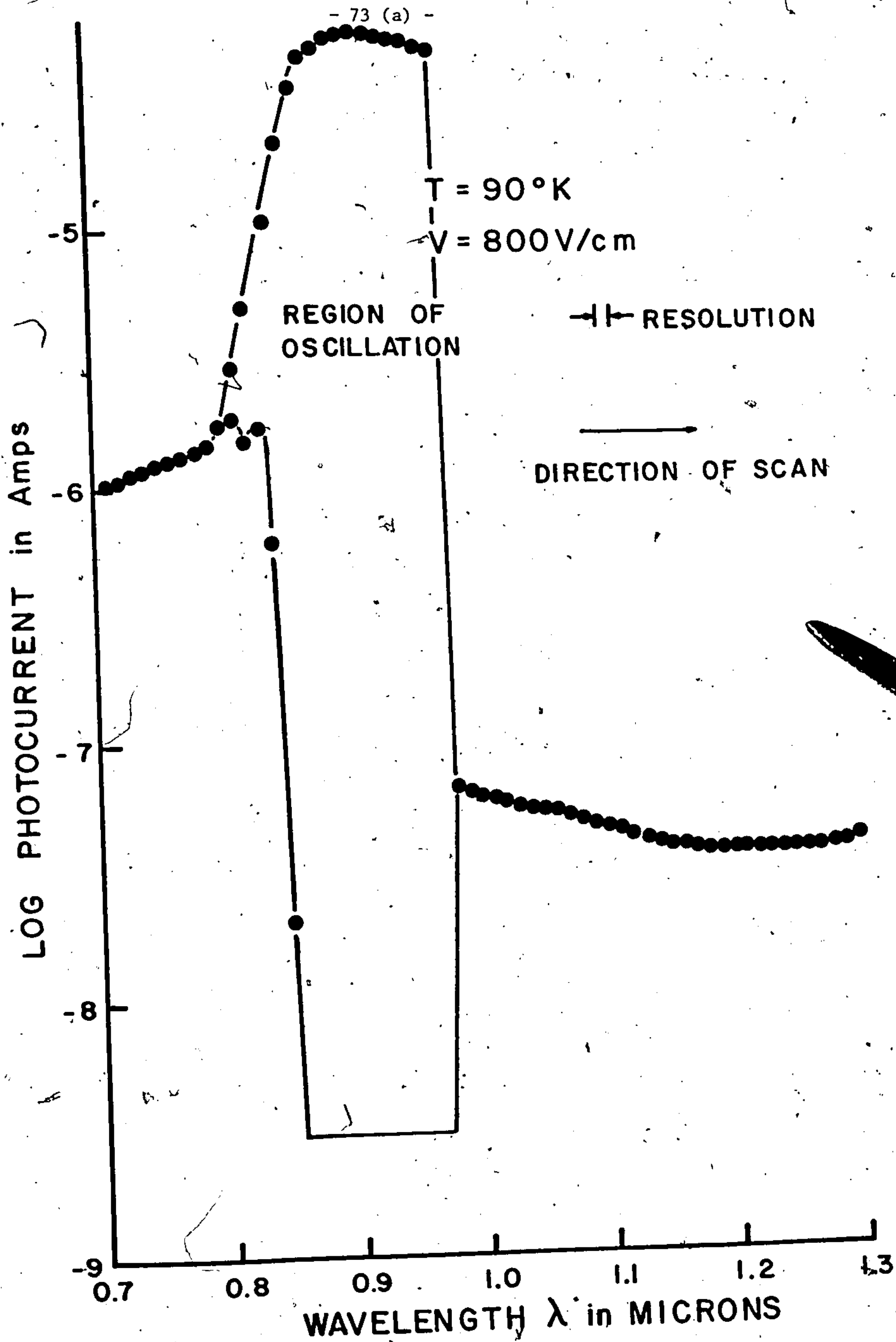
T = 90°K
V = 800V/cm
REGION OF OSCILLATION
RESOLUTION
DIRECTION OF SCAN
LOG PHOTOCURRENT in Amps
-5
-6
-7
-8
-9
0.7
0.8
0.9
1.0
1.1
1.2
1.3
WAVELENGTH λ in MICRONS

thought to be due to both sensitizing and memory effects in the material, and forms the subject of another work (72P4).

3.1.4 Electric Field

Fig. 4-16 illustrates the behaviour of the frequency of oscillations as the applied electric field was varied at 300°K in the dark. The results at 90°K under 0.90μ illumination were similar.

The relationship is superlinear, and clearly indicates that the frequency of oscillation is field dependent. This also shows that the capture rate is field-dependent, since the frequency will be determined by the capture rate (for fixed values of temperature and carrier concentration, as is the case here).

As derived in the Appendix, the capture rate must increase more rapidly than the square root of the field if F.D.T. is to take place. As Fig. 4-16 illustrates, this condition is satisfied here.

3.2 Quenching

3.2.1 Optical Quenching

As mentioned in section 3.1.3, if a spectral scan was performed at high fields at 90°K, the oscillations would self-quench for wavelengths above 0.96μ, as illustrated in Fig. 4-15. A series of scans, begun at both ends of the spectrum (0.70μ, and 1.60μ) yielded similar results.

If a particular scan was begun at the high energy end of the spectrum (at 90°K and for an applied field of 800 V/cm), the oscillations would be generated by radiation in the 0.86μ to 0.96μ range. If the wave-

Fig. 4-16 Frequency of Oscillation as a Function of Applied Electric Field at 300°K

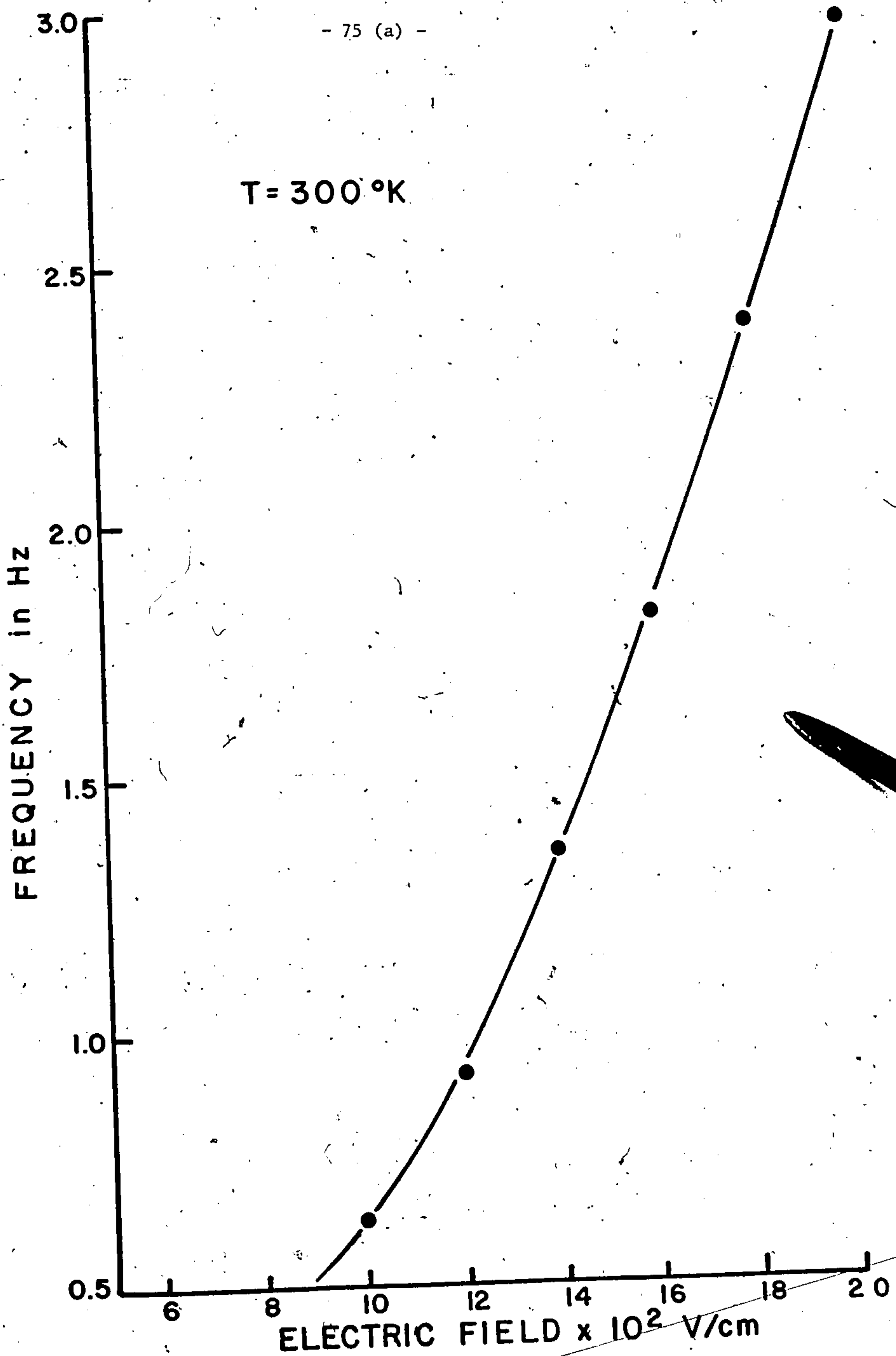
T = 300 °K
FREQUENCY in Hz
3.0
2.5
2.0
1.5
1.0
0.5
6
8
10
12
14
16
18
20
ELECTRIC FIELD x $10^2$ V/cm

length was increased past 0.96μ, both the oscillations and the photocurrent were quenched.

When scanning started from the low energy end (1.60μ), the oscillations were generated by radiation of wavelengths ∿ 1.43μ to ∿ 1.26μ. In this case the oscillations were very irregular. At lower wavelengths than 1.26μ, the oscillations and the photocurrent were again quenched.

After the oscillations ceased, they could not subsequently be regenerated at that temperature at any wavelength.

The oscillations would be generated by the 0.84μ to 0.96μ radiation because of the large number of carriers that are generated in this range of wavelengths, as illustrated in Fig. 4-7. The oscillations could also be generated by the 1.28μ radiation because of the presence of an impurity level 0.54 eV above the valence band. This would hold especially true if the level was heavily populated, as the size of the peak in Fig. 4-6 seems to indicate. As well, the peak is rather wide so that there exists an energy range over which carriers are generated.

The most significant aspect of these spectral scans was the fact that both the oscillations and the photocurrent were quenched once the sample was illuminated with radiation in the 1.00μ to 1.20μ range. This effect can be explained by assigning a real meaning to the large valley centered around 1.16μ as illustrated in Fig. 4-6.

The GaAs contains an impurity level 0.45 eV above the valence band, or 1.06 eV (1.16μ) below the conduction band. The level is composed of r centres, that is sensitizing centres, that are partly filled and thus negatively charged due to the compensation of the material. These centres

thus act so as to make the material highly photo sensitive at 90°K for 0.90μ radiation as was explained in section 2.3.1. As well, due to the negative charge of the centre, it presents a repulsive barrier to free charge carriers (electrons). The free charge carriers, however, may become trapped at the centre if they are "heated" so that they have sufficient energy to overcome the potential barrier. The energy is provided by a high electric field, and the effect is F.D.T. Current oscillations thus result.

If the wavelength of the incident radiation is changed to 1.16μ both the current oscillations and the photocurrent are quenched. This is due to the fact that the radiation empties the r centres. As a result, the repulsive barrier is no longer present and the F.D.T. mechanism ceases to be operative. As well, since the electrons formerly in the r centres recombine in the fast s centres, there are few free carriers and the photoconductivity drops. No wavelength (in the range considered) can generate the oscillations since the 0.45 eV level is now empty and the F.D.T. effect cannot take place.

It has been mentioned that the current oscillations were quenched for temperatures below ∿ 125°K by the 1.16μ radiation. If the sample was heated to above ∿ 125°K, the oscillations could be regenerated (with the proper wavelength of illumination). Since ∿ 125°K corresponds to the temperature at which the hole demarcation level crosses the level containing the r centres and thus allows the level to be "refilled", then this this again indicates that the 0.45 eV level must be at least partly filled to generate oscillations. As well, it explains why the temperature

of the sample had to be increased subsequent to a quenching run if the oscillations were to be regenerated.

3.2.2 Thermal Quenching

The second manner in which the oscillations could be quenched was by changing the temperature of the sample.

For oscillations generated by 0.90μ radiation at 90°K, the quenching occurred if the temperature of the sample was increased above 225°K. For oscillations generated in the dark at 300°K, the quenching would occur when the temperature was decreased.

The exact temperature at which the oscillations ceased in the dark could not be determined since, as the temperature was decreased, they could be regenerated by increasing the field. However, in the temperature range ∿ 275°K to ∿ 225°K, no oscillations could be observed either in the dark or with illumination of 0.90μ wavelength. The reason for this behaviour is not known.

Note, however, that the temperature range ∿ 275°K to ∿ 225°K corresponds to the break in the temperature dependence of the dark current from the 0.12 eV activation energy to the 0.70 eV activation energy in Fig. 4-3. This temperature range also corresponds to the change in photoconductivity from decreasing to increasing value (with rising temperature) for the three wavelengths illustrated in Fig. 4-8. A more intensive investigation of the current oscillations in the temperature range ∿ 225°K to ∿ 275°K would be in order if the exact mechanism involved in this particular range is to be understood.

### 3.2.3 Quenching by a Second Source

In the two source optical quenching study of the GaAs samples, the oscillations were generated at 90°K using a 0.90μ source and were quenched with radiation from a second source. While the investigation of this effect was extensive, the results obtained were quite simple.

In scanning with the quenching source from both low and high energy ends, the results were similar; the oscillations were quenched for incident radiation in the (1.16 ± 0.03)μ range. Attempts to quench the oscillations with radiation of other wavelengths from 0.70μ to 2.00μ failed.

The interpretation of the results is consistent with the previous arguments. 1.06 eV (1.16μ) radiation empties the slow r centres (sensitizing centres) and the carriers recombine at the fast s centres. This prevents the r centres from acting effectively in the F.D.T., which prevents the necessary current drop for N.D.R. to be created.

As for the one source experiment, the photocurrent was quenched here as well. In this case however, it was possible to see if quenching occurred first for the oscillations or the photocurrent.

In all cases the oscillations would disappear first, and the photocurrent would then decrease with a fairly fast decay time. This means that the oscillations did not disappear because the free carriers concentration was too small ($n\ell$ product too small to form domains), a factor that would have to be considered when only one source is used. Instead, the oscillations cease because the 0.45 eV level has been emptied and F.D.T. no longer occurs at the r centres. The decrease in the photocurrent was not as large as for the one source experiment since in this case the 0.90μ

source still provides impurity photoconduction.

Thus the results of the two source experiments further indicate that the 0.45 eV level is the one responsible for the F.D.T. mechanism.

IV-4 Summary of Results

The main results obtained in this investigation of semi-insulating GaAs:Cr are presented in tabular form on the following two pages.

Table 4-2 lists the impurity levels found in GaAs in this investigation, both at 300°K and 90°K. As well, the methods by which the levels were found are mentioned. The fourth column contains the levels that have been identified by other authors, and the next column indicates the impurity believed to be responsible for the level. Finally, the references for these levels are given.

It can be seen from this Table that the emphasis in this work was on identification of the level responsible for F.D.T., which was found to be 0.45 eV above the valence band.

All values of energy in Table 4-2 are measured from the top of the valence band.

Table 4-3 summarizes some of the characteristics of the three main types of oscillatory phenomena that has been observed in GaAs. The fourth column lists the characteristics of the oscillations studied in this work.

The similarities between the characteristics obtained here and the slow domains (column 3) clearly indicates they are due to the same effect: F.D.T.

Table 4-2 Impurity Levels in GaAs as Found in This Work

| Energy Level eV | Temp. °K | Method of Identication | Reported Values eV | Impurity Responsible | References |
|---|---|---|---|---|---|
| 1.36 | | Postulated | 0.158 | Cr, Cu | 66B1, 66S2 |
| 0.79 | 300 | Temperature Variation of Current | 0.79 | Cr | 68A1, 68H1, 70K1, 71G1, 71K1, 72P1, 72P2, 73A1. |
| 0.54 | 90 | Spectral Scan | 0.54<br>0.5<br>0.56 | Co ?<br>Cu<br>Lattice Defect | 66F1<br>69V1, 69S1<br>71K1 |
| 0.45 | 90 | Spectral Scan | 0.45 | Lattice Defect | 61B1, 62B2, 64B1 |
| (0.4 ) | ( 100) | Optical Quenching<br>Temp. Quenching | 0.43-0.51<br>0.39-0.45 | Lattice Defect Sensitizing | 72B2, 72P3<br>72B1 |
| | | | 0.48 | ? | 70H1 |
| 0.42 | 300 | Spectral Scan | 0,42 | Cu ? | 61B1 |
| 0.15 | 90 | Spectral Scan | 0.15 | Cu | 64B1, 66S1, 66S2 |
| 0.12 | 225 | Temperature Variation of Current | 0.1<br>0.13 | Cu<br>Cu | 71G1<br>61B1 |
| 0.09 | 100 to 225 | Temperature Variation of Current | 0.09 | Cu<br>Sensitizing ? | 61B2, 72P1, 61B1, 64B1 72P3 |

Table 4-3 Characteristics of Three Types of Oscillations in GaAs (72T1)

| Property | Gunn Effect | Acoustoelectric Effect | Field Dependent Trapping | Present Work |
|---|---|---|---|---|
| Sample Orientation | arbitrary | <110>, (<111>) | Arbitrary | Arbitrary |
| Threshold Field | 3,000 V/cm | 800 V/cm | 200 - 2,000 V/cm | 750-950 V/cm |
| Domain Velocity | $1 \times 10^7$ cm/sec | $3.0 \times 10^5$ cm/sec | $10^{-1} - 10^5$ cm/sec | $10^{-1} - 10^2$ cm/sec |
| Minimum $n\ell$ Product | $> 10^{12}$ cm$^{-2}$ | $\sim 10^{15}$ cm$^{-2}$ | $\sim 10^7 - 10^{13}$ cm$^{-2}$ | $\sim 10^7 - 10^9$ cm$^{-2}$ |
| Frequency of Oscillations (Range) | $> 10^7$ Hz | $\sim 10^5$ Hz | $10^{-1} - 10^5$ Hz | 0.5 - 800 Hz |

# CHAPTER V CONCLUSION

A study was made of some of the electrical and optical properties of semiinsulating GaAs:Cr (at $90^{o}K$ in particular). The GaAs exhibited anomalous behaviour under $0.90\mu$ radiation and high field conditions: current oscillations occurred, primarily for temperatures below $225^{o}K$ and for applied fields greater than 750 V/cm.

1 - The cause of the current oscillations was discussed in terms of a number of possible effects that have been proposed by other workers. Of these, the Gunn effect and the acousto-electric effect, two of the three main effects, were rejected, primarily due to the high frequency of the oscillations they normally exhibit ( > $10^{5}$ Hz), as compared to the low values obtained in this study (1 Hz to 100 Hz). As well, these mechanisms require a minimum $n\ell$ product for domain formation that was much higher ($\sim 10^{15}$ $cm^{-2}$) than the values found in this work ($\sim 10^{7} - 10^{9}$ $cm^{-2}$). This left Field Dependent Trapping as the mechanism responsible for the oscillations.

2 - The semi-insulating GaAs exhibited non-ohmic behaviour at $300^{o}K$ in the dark for high applied electric fields, oscillatory behaviour occuring for fields greater than 950 V/cm. At $90^{o}K$, under the influence of $0.90\mu$ radiation, the threshold voltage needed to generate the oscillations was 750 V/cm. At this temperature in particular, the current-voltage characteristics exhibited a region of Negative Differential Resistivity due to Field Dependent Trapping of carriers.

3 - The optical measurements yielded a number of impurity levels in the material, in particular one 0.45 eV above the valence band. A second level 0.15 eV above the valence band was found to be responsible for a high photocurrent at low temperatures. The role of this level was explained in terms of a model based on double excitation. As well as the 0.15 eV level, the model contained a 1.36 eV level and two recombination centres: a fast s centre whose energy value of could not be determined, and a slow r centre corresponding to the 0.45 eV level. Subsequent behaviour of the sample was explained using these energy levels.

4 - The 0.45 eV level was found to exhibit properties that indicated it was both the compensating level and the level responsible for F.D.T. of the free charge carriers. Infrared quenching of the oscillations by 1.16μ radiation, as well as self-quenching near this wavelength, were used to show that the emptying of the 0.45 eV level stopped the current oscillations by preventing F.D.T. of electrons from taking place in a large enough number to create a region of N.D.R. in the sample. This meant that the 0.45 eV level had to be partly filled if F.D.T. was to occur. By using the frequency behaviour of the oscillations, a height of 0.30 eV was proposed for the repulsive Coulomb barrier surrounding the 0.45 eV level.

5 - It was found that successful observation or annihilation of the oscillations was critically dependent on the carrier concentration. The nature of the compensation, on the other hand, seems to have little importance on being able to generate the oscillations. Current oscillations have been observed in high resistivity GaAs compensated with many different agents (61B1, 63B1, 66K1, 69V2, 69S1). The level responsible for the current oscillations found in this work was due to a lattice defect in the material.

Optical quenching of the oscillations could be carried out on GaAs compensated by different means. This would determine whether or not the level responsible for the oscillations is a native defect. Hall measurements in the oscillatory regime would be in order to ascertain the type of charge carrier and type of conduction present during the oscillations. This presents problems, however, due to the high resistance of the material needed to have the effect and due to the fact that the domains are in motion.

6 - A number of practical applications stemming from the oscillatory behaviour of the material can be envisioned. One such application would be in long time delay lines. This area uses the low frequency of the oscillations for its main parameter. Because of the high photo-sensitivity of the material, signals could be triggered optically. Work in this area is already being done (72T1). In its simplest form, the material could be used as an oscillator in the 1 Hz region, with the applied field controlling the frequency. However, foremost in importance is a thorough knowledge of these low frequency effects in GaAs so that a method of controlling them can be devised. This is of particular interest since these oscillations cause instabilities in Gunn devices. Work in this area is already in progress (73T1).

# APPENDIX FIELD DEPENDENT TRAPPING

## A Effect of Change of Capture Rate on Carrier Concentration

Field Dependent Trapping, as originally proposed by Ridley and Watkins (61R1, 61R2, 61R3) requires that the capture rate of repulsive centre change with applied field (above a threshold value). The behaviour of the capture rate of a repulsive centre will be considered in more detail in this Appendix.

Consider an extrinsic n-type semiconductor whose conduction electrons at low temperature are due to thermal ionization of a negatively charge impurity centre. For simplicity, it shall be assumed that several kT separate any other localized levels which may exist in the material, and that the Fermi level is near the impurity centre under discussion. Thus, other localized levels do not interact significantly with the conduction band. These conditions are met by the heavily compensated GaAs used in this work.

For the above conditions, the density of free electrons is governed only by the rate of transition associated with the negatively charged impurity level. The rate of increase of electron density, n, in the conduction band would be the number of electrons thermally ionized to the band minus the number of electrons thermally captured by the level; or

$$\frac{dn}{dt} = gN^{-} - BnN^{o} \quad (1)$$

where $n$ density of electrons in the conduction band

$N^-$ density of filled levels

$N^o$ density of unfilled levels

$g$ thermal ionization rate

$B$ thermal capture rate

$g$ and $B$ are averaged over the electron distribution and are in general field dependent.

If one denotes thermal equilibrium (low field) values by the suffix O, the above equation becomes

$$\frac{dn}{dt} = g_o N_o^- - B_o n_o N_o^o = 0 \qquad (2)$$

or

$$g_o = B_o \frac{N_o^o}{N_o^-} n_o$$

$$= B_o n_1$$

where

$$n_1 = 2\left\{ \frac{2\pi m^* kT}{h^2} \right\}^{3/2} \exp\left(-\frac{E_t}{kT}\right) \qquad \text{(59S1)} \quad (3)$$

and $E_t$ is the energy of the level measured from the conduction band edge.

Since the thermal ionization rate depends solely on the lattice temperature, it will be assumed that it is not appreciably affected by the field. At the steady state, therefore, (2) becomes

$$B_o n_1 N^- - BnN^o = 0 \qquad (4)$$

If $\Delta n$ is the increase in electron density due to the field, then

$$n = n_o + \Delta n$$

$$N^- = N_o^- - \Delta n$$

$$N^o = N_o^o + \Delta n$$

Replacing these values in (4) and simplifying, one has

$$\Delta n = \tfrac{1}{2}[\{(N_o^o + n_o + \gamma n_1)^2 - 4n_o N_o^o(1-\gamma)\}^{\frac{1}{2}} - (N_o^o + n_o + \gamma n_1)] \qquad (5)$$

where

$$\gamma = \frac{B_o}{B} \qquad (6)$$

or $\gamma$ is the ratio of thermal capture rates at low to high field. For negative resistance then, a necessary condition is that

$$B > B_o \quad \text{or} \quad \gamma < 1 \qquad (7)$$

Equation (5) may be simplified where the doping is such that only about half the levels would be occupied at $0^oK$, that is, the level under consideration is partly filled. Thus, there is always a substantial density of unoccupied levels available for electron capture, as was the case in the GaAs used in this work. At temperatures less than that needed for

complete ionization of the level, the electron density in the conduction band (low field conditions) is much less than the density of unfilled levels (high resistivity material) or

$$n_o < n_1 << N_o^o \qquad (8)$$

For a repulsive centre $\gamma < 1$ and thus $\gamma n_1$ is small, and (5) becomes after simplification

$$\Delta n = -n_o(1 - \gamma) \qquad (9)$$

Since $\gamma < 1$, then $(1 - \gamma)$ will always be a positive number; as a result $-n_o(1 - \gamma)$ will always be negative, and so will $\Delta n$. Thus the high field changes the thermal capture rate (for repulsive centres) so as to produce a decrease in electron density in the conduction band, and thus negative conductivity (N.D.R.).

B. Field Dependence of the Capture Rate

One may obtain the condition for negative resistance by considering the differential conductance which is given by

$$\frac{dG}{dF} = e\left(\mu_a \frac{dn_b}{dF} + \mu_b \frac{dn_b}{dF}\right) + e\left(n_a \frac{d\mu_a}{dF} + n_b \frac{d\mu_b}{dF}\right) \qquad (10)$$

where $G$ conductance

$F$ electric field

$\mu_a$ mobility of free electrons

$n_a$ density of free electrons

$\mu_b$ mobility of trapped electrons

$n_b$ density of trapped electrons

In this case $\mu_b = 0$ since the electrons are trapped, and

$$n_a = n_o + \Delta n$$

so that (10) becomes

$$\frac{dG}{dF} = e\{ \mu_a \frac{d\Delta n}{dF} + (n_o + \Delta n) \frac{d\mu_a}{dF} \} \qquad (11)$$

Now one must assume that the free electrons mobility $\mu_a$ is proportional to some power p of the electric field F, where the field exponent p is a function of the scattering mechanism. In this case $\mu_a \propto F^p$ and substituting in (11) yields

$$\frac{dG}{dF} = \frac{e\, \mu_a (n_o + n)}{F} \quad \{ \frac{F}{n_o + \Delta n} \cdot \frac{d\Delta n}{dF} + p \} \qquad (12)$$

The relationship between current density J, field F, and conductance G is given by

$$J = GF \qquad (13)$$

and the condition for negative resistance is

$$\frac{dJ}{dF} < 1$$

which becomes, upon substituting (13)

$$\frac{-\frac{dG}{dF}}{\frac{G}{F}} > 1 \tag{14}$$

Substituting expression (12) in (14) and simplifying, one obtains the condition for negative resistance as:

$$-\frac{F}{n_o + \Delta n} \cdot \frac{d\Delta n}{dF} - p > 1 \tag{15}$$

For the case of repulsive centres, one had that

$$\Delta n = - n_o(1 - \gamma) \tag{9}$$

and

$$\gamma = \frac{B}{B_o} \tag{6}$$

Substituting for $\Delta n$ in (15) and simplifying finally yields

$$\frac{F}{B}\,\frac{dB}{dF} - p > 1 \tag{16}$$

It can be seen from equation (16) that the field exponent p, a function of the scattering mechanism, should be negative and large to obtain

negative resistance. This makes impurity scattering undesirable since when it is dominant the mobility rises with increasing field and thus p is positive. When lattice scattering is dominant, however, p is negative and will depend on the lattice and carrier temperature. At constant lattice temperature, the most demanding case, that of acoustic phonon collision scattering, has the drift velocity of the electrons proportional to the negative square root of the applied field, and thus $\mu_a \propto F^{-\frac{1}{2}}$ and $p = -\frac{1}{2}$. In this case the above condition (16) is satisfied if the capture rate increases more rapidly than the square root of the field; that is, (16) may be written, using $p \doteq -\frac{1}{2}$

$$\frac{F}{B}\,\frac{dB}{dF} > \frac{1}{2} \tag{17}$$

and

$$B > \sqrt{F}$$

C Magnitude of the Potential Barrier

The first requirement in calculating the height of the potential barrier present at a repulsive centre is an estimate of the electron density near the centre, since this will be the governing factor in determining the effective rate of capture. For this, one needs to know the precise potential field around the centre; that is, one needs a refined picture of deep-level centres in semiconductors, which is not available. One can circumvent

this problem if it is assumed that the electron density near the centre differs from the average by a factor

$$e^{-\frac{\phi}{kT}}$$

at thermal equilibrium (51P1). $\phi$ is the potential barrier. Now if $\beta$ is the capture rate of electrons which have surmounted the barrier, the effective capture rate $B_o$ will differ from $\beta$ by the factor $\exp(-\phi/kT)$, or

$$B_o = \beta e^{-\frac{\phi}{kT}} \qquad \text{Low Field} \qquad (18)$$

Now if $\phi > kT$, then the main variation in capture rate with field will come from the density factor, as required for N.D.R. For "hot" electrons, the distribution function (18) changes in general from a Maxwellian ($B_o$ is the low field value) to some function of the field and potential barrier, or $f(F, \phi)$. If one assumes $\beta$ varies little with field, (18) becomes

$$B = \beta f(F, \phi) \qquad \text{High Field} \qquad (19)$$

For potential barriers greater than kT, the term which varies most rapidly with field will probably be the distribution function $f(F, \phi)$ In the region of field strength where $p = -\frac{1}{2}$, to a reasonable approximation the distribution function $f(F, \phi)$ is of the form

$$f(F, \varepsilon) = e^{-a\left(\frac{\varepsilon}{kT_e}\right)^2} \qquad \text{(54Y1)} \qquad (20)$$

where $\varepsilon$ electron energy

$T_e$ electron temperature

$a = 0.243$

The value of a is obtained by defining the mean kinetic energy of the electrons as $3/2\ kT_e$. In this case, the electron temperature $T_e$ is proportional to the field strength F so

$$T_e = \text{const.} \times F$$

Thus, using (20), (19) becomes

$$B = \beta e^{-0.243\left(\frac{\phi}{kT_e}\right)^2}$$

and the condition for negative resistance, (11) becomes

$$\frac{F}{e^{-0.243\left(\frac{\phi}{kT_e}\right)^2}} \frac{d e^{-0.243\left(\frac{\phi}{kT_e}\right)^2}}{dF} > 0.5 \qquad (21)$$

After simplification , (21) reduces to

$$0.486 \left\{\frac{\phi}{kT_e}\right\}^2 > 0.5$$

and thus

$$\frac{\phi}{kT_e} > 1.01$$

Since the mean energy of hot electrons is roughly three to four times the thermal equilibrium mean energy in this region (69S2), an approximate condition is

$$\frac{\phi}{kT} > 4$$

Assuming that the lattice temperature is low enough so that $kT < 0.02$ eV, the barrier height for F.D.T. becomes

$$\phi > 0.08 \text{ eV}$$

# REFERENCES


51P1 Pekar S. T., Abb. Low Phys. 1, 47 (1951)

52M1 Moss T. S., "Photoconductivity in the Elements", Butterworth, London (1952), p. 30

54S1 Shockley W., Bell System. Tech. J. 33, 799 (1954)

54Y1 Yamashita J. and Watanabe M., Prog. Theor. Phys. 12, 443 (1954).

55B1 Baum R. M. and Battley J. F., Phys. Rev. 98, 923 (1955).

56S1 Shulman R. G. and Wyluda B. J., Phys. Rev. 102, 1455 (1956).

57W1 Weinreich G., Phys. Rev. 107, 317 (1957)

59B1 Boer K. W., Z. Physik 155, 184 (1959).

59K1 Kroemer H., Proc. I.R.E. 47, 397 (1959)

59S1 Smith R. A. "Semiconductors", Cambridge University Press, London (1959), p. 78

59W1 Weisberg L. R., Rosi F. D., and Herkart P. G., in "Properties of Elemental and Compound Semiconductors" (Inter-Science Publishers, Inc., New York (1959)). Vol. V of Metallurgical Society Conferences, p. 25-65.

60B1 Bube R. H., "Photoconductivity of Solids", Wiley (1960), p. 53-55, 64-68, 335-356.

60J1 Johnston L. and Levinstein H., Phys. Rev. 113, 1191 (1960).

61B1 Blanc J., Bube R. H., and MacDonald H. E., J. Appl. Physics 32, 1666 (1961).

61B3 Boer K. W., J. Physics Chem. Solids 22, 123 (1961)

61R1 Ridley B. K. and Watkins T. B., J. Phys. Chem. Solids 22, 155 (1961).

61R2 Ridley B. K. and Watkins T. B., Proc. Phys. Soc. Lond. 78, 293 (1961)

61R3 Ridley B. K. and Watkins T. B., Proc. Phys. Soc. Lond. 78, 710 (1961).

62B2 Bube R. H. and MacDonald H. E., Phys. Rev. 128 2062 (1962)

62H2 Hilsum C., Proc. I.R.E. 50, 185 (1962).

62S2 Smith R. W., Phys. Rev. Lett. 9, 87 (1962).

63B1 Barraud A., C R Acad. Sci. (France) 256, 3632 (1963)

63E1 Erlbach E., Phys. Rev. 132, 1976 (1963)

63R1 Ridley B. K., Proc. Phys. Soc. 82, 954 (1963).

64B1 Blanc J., Bube R. H., and Weisberg L. R., J. Phys. Chem. Solids, 25, 225 (1964).

64B2 Beale J. R. A. and Pomerantz M., Phys. Rev. Letters (USA) 13, 198 (1964).

64G1 Gunn J. B., I.B.M. Journal 8, 141 (1964).

64N1 Northrop D. C., Thornton P. R., and Trezise K. E., Solid-State Electronics 7, 17 (1964).

65B4 Boer K. W., Phys. Rev. 139, A 1949 (1965)

65K1 Kroemer H., Proc. I.E.E.E. 53, 1246 (1965)

65R2 Ridley B. K. and Pratt R. G., J. Phys. Chem. Solids 26, 21 (1965)

65S1 Sliva P. O. and Bray R., Phys. Rev. Letters (USA) 14, 372 (1965)

65S2 Smith A. W., Solid St. Electron. 8, 833 (1965).

65W1 Wang W. C., Appl. Phys. Letters (USA) 6, 81 (1965)

66B1 Basinski J., Can. J. Phys. 44, 941 (1966)

66F1 Fistul' V. I. and Agaev A. M., Sov. Phys. - Solid State 7, 2975 (1966).

66H1 Hayakawa H., Kikuchi, M., and Abe Y. Japan J. Appl. Phys. 5, 734 (1966).

66K1 Karkhanin Yu. I. and Tretyak O. V., Sov. Phys. - Solid State 7, 2787 (1966).

66K2 Kikuchi M., Hayakawa H., and Abe Y., Japan J. Appl. Phys. 5, 735 (1966).

66M1 McCumber D. E. and Chynoweth A. G., I.E.E.E. Trans. Electron Devices ED-13, 4 (1966).

66S1 Shirafuji J., Japan J. of Appl. Physics. 5, 469 (1966).

66S2 Stunders I. J. and Crede R. H., Priv. Comm. (1966)

66W1 Willardson R. K. and Beer A. C.: Editors "Semiconductors and Semimetals, Vol. 1, p. 148 Academic Press, New York and London (1966)

67K1 Kikuchi M., So. St. Comm. 5, 855 (1967).

67K2 Kurova I. A., Vrana M., and Vavilov V. S., Sov. Phys. - Solid State 8, 1892 (1967).

67S1. Sugiyama K., Japan J. of Appl. Physics 6, 601 (1967).

67T1 Tokumaru Y. and Kikuchi M., Japan J. Appl. Phys. 6, 654 (1967).

68A1 Allen G. A., Brit. J. Appl. Phys. 1, Series 2, 593 (1968).

68H1 Heath D. R., Selway P. R., and Tooke C.C., Brit. J. Appl. Phys. 1, Series 2, 29 (1968).

68S1 Shirafuji J., Solid-State Electronics 11, 983 (1968).

68S2 Senechal R. R. and Basinski J., J. Appl. Phys. 39, 4581 (1968).

68S4 Schmidlin F. W. and Roberts G. G., Phys. Rev. Letters 20, 1173 (1968).

68T1 Tokumaru Y. and Kikuchi M., Japan J. Appl. Phys. 7, 95 (1968).

69I1 Inoue T. and Ohyama M., Japan J. Appl. Phys. 8, 1363 (1969).

69M1 Milner-Brown H. and Fortin E., Can. J. Phys. 47, 2789 (1969).

69M2 Milner-Brown H., M.Sc. Thesis, University of Ottawa, (1969).

69S1 Shirafuji J., Japan J. Appl. Phys. 8, 898 (1969).

69S2 Sze S. M., "Physics of Semiconductor Devices", J. Wiley & Sons, New York (1969), p. 57.

69T2 Tokumaru Y., Japan J. Appl. Phys. 8, 76 (1969).

69V1 Viehmann W., Appl. Phys. Letters 14, 39 (1969).

69V2 Vorob'ev Yu. V., Karkhanin Yu. I., and Tretyak O. V., Phys. Stat. Sol. 36, 499 (1969).

69V3 Volkov A. F. and Kogan Sh. M. Sov. Phys. Uspekhi 11, 881 (1969).

70F1 Fortin E., Rev. Sci. Instruments. 41, 1252 (1970).

70H1 Hasegawa F., Japan J. Appl. Phys. 9, 638 (1970).

70K1 Kolchanova N. M., Nasledov D. N., Mirdzhalilova M. A. and Ibrajimov V. Yu., Sov. Phys. - Semicond. 4, 294 (1970).

70L1 Lenczewski P. and Fortin E., Phys. Stat. Sol. (a) 3, K 267 (1970).

70T1 Tokumaru Y., Japan J. Appl. Phys. 9, 95 (1970).

70T2 Tretyak O. V., Sov. Phys. - Semicond. 4, 517 (1970).

71G1 Gontar' V. M., Egiazaryan G. A., Rubin V. S., Murygin V. I., and Stafeev V. I., Sov. Phys. - Semicond. 5, 939 (1971).

71K1 Kornilov B. V., Vil'kotskii V. A., Aleksandrova G. V., Tereshko G. N., and Tsarevskaya T. P., Sov. Phys. - Semicond. 5, 119 (1971).

71V1 Vorob'ev Yu. V., Karkhanin Yu. I., and Tretyak O. V., Sov. Phys. - Semicond. 5, 254 (1971).

72B1 Brodovoi V. A. and Derikot N. Z., Sov. Phys. - Semicond. 6, 237 (1972).

72B2 Brodovoi V. A. and Peka G. P., Sov. Phys. - Sol. St. 13, 2015 (1972).

72P1 Peka G. P. and Karkhanin Yu. I., Sov. Phys. - Semicond. 6, 261 (1972).

72P2 Peka G. P. and Karkhanin Yu. I., Sov. Phys. - Semicond. 6, 639 (1972).

72P3 Prat F. and Fortin E., Can. J. Phys. 50, 2551, (1972).

72P4 Prat F. G. P., M.Sc. Thesis, University of Ottawa, (1972).

72T1 Tokumaru Y. and Mikoshiba N., Japan J. Appl. Phys. 11, 678 (1972).

73A1 Alebsandrova G. A., Zavadskii Yu. I., Kornilov B. V., and Skvortsov I. M., Sov. Phys. - Semicond. 6, 1170 (1973).

73T1 Teszner J. L., J. Appl. Phys. 44, 2765 (1973).